# Noradrenergic and Arousal Dynamics During Sleep and Psychedelic (DOI)-Induced States

by

TAPLEY SORENSON

A THESIS

Presented to the Department of Neuroscience
and the Robert D. Clark Honors College
in partial fulfillment of the requirements for the degree of
Bachelor of Science

May 2025

# An Abstract of the Thesis of

Tapley Sorenson for the degree of Bachelor of Science
in the Department of Neuroscience to be taken June 2025

Title: Noradrenergic and Arousal Dynamics During Sleep and Psychedelic (DOI)-Induced States

Approved: *David McCormick, Ph.D.*
Primary Thesis Advisor

Approved: *Nicole Dudukovic, Ph.D.*
Clark Honors College & Neuroscience Honors Faculty Representative

Approved: *Evan Vickers, Ph.D.*
Second Reader

This project presents a multi-phase experimental pipeline to facilitate the exploration of natural sleep and psychedelic-induced arousal states in head-fixed mice utilizing electrophysiology, pharmacology, and mesoscopic calcium imaging. During Phase 1, we established that mice could undergo natural sleep on a behavior rig while head-fixed using pilot electromyography (EMG) and intracranial electroencephalography (iEEG) implants. These recordings were then used to classify arousal states through manual sleep scoring to lay the foundation for further investigations of electrophysiological states. Phase 2 explored the arousal state induced by the psychedelic 2,5-Dimethoxy-4-iodoamphetamine (DOI) and the ~0.03 Hz infra-slow pupil oscillation that it has been demonstrated to consistently elicit by the McCormick Lab. Given that infra-slow pupil oscillations are also observed during NREM sleep, we investigated whether the arousal state induced by DOI is electrophysiologically distinct from the NREM state. EMG and iEEG analysis revealed that the DOI-induced state paradoxically

contains both sleep-like and wake-like features. During Phase 3, mesoscopic two-photon calcium imaging was carried out to examine noradrenergic activity before and after the administration of DOI. Although the infra-slow oscillation did not emerge during this session, it does confirm the viability of using two-photon mesoscopic calcium imaging to assess noradrenergic axonal activity during the DOI-induced state in a preparation that allows for concurrent EMG and EEG recordings. Altogether, the three phases of this project offer a framework for studying novel brain states and their underlying behavioral, electrical, and neurophysiological signatures.

## Acknowledgements

I would first and foremost like to express my overwhelming gratitude to the members of my thesis committee: David McCormick, whose leadership and commitment to both rigorous research and collective wellbeing has instilled in me the essential understanding that research is truly "we-search"; Nicole Dudukovic, whose guidance and support has shaped my time here at the UO and continues to inspire my future aspirations; and Evan Vickers, who went above and beyond after unexpectedly stepping in to be my primary guide for this project. I am so thankful for your direction and feel incredibly fortunate to be able to consider you all as mentors.

I would also like to thank the members of the McCormick Lab. I have gained so much these last three years by being able to witness and participate in this intellectually and interpersonally rich research environment. Thank you to lab members Daniel Hulsey, Brett Emannuel, Mary Janusevskis, Jeremy Guenza-Marcus, Joe Wargo, Kat Nueweiler, Sophia Calevi, Chase Berryman, Tanner Rozendal, and Liz Riebe, as well as lab alumni Kevin Zumwalt, Lindsey Collins, Laura Boddington, and Katelyn McCallister.

I would be remiss not to acknowledge the UO professors and faculty who have introduced me to paradigm-shifting concepts and been guiding lights during my undergraduate degree. Thank you, in no particular order, to Dare Baldwin, Gantt Gurley, Avinash Singh, Paige Haagen, Tobin Hansen, Chanel Meyers, Barbara Mossberg, Miriam Jordan, Paul Dassonville, Robin Hopkins, Nicki Swann, Amy Costales, Paulo Henríquez, Jesús Sepúlveda, and Caitlin Fausey. Additionally, I would like to thank Karl Reasoner and the Office of the Vice President for Research and Innovation for supporting this research project.

Last but by no means least, thank you to my loved ones for your encouragement, reassurance, and levity throughout the course of this thesis. I am but a mosaic of all of you.

# Table of Contents

# List of Figures

# List of Tables

# Introduction

Neurons, the fundamental units of the brain and the nervous system at large, communicate and transmit information electrochemically (del Castillo & Katz, 1954; Hodgkin & Katz, 1949; Loewi, 1956). The electrical excitability of neurons, coupled with the movement of ions and the activity of chemical messengers called neurotransmitters, ultimately give rise to the electrical activity governing the complex functions and behaviors that are understood to be within the brain's control (Catterall, 1984). The synchronization of the electrical activity of neurons produces rhythmic fluctuations in voltage across the brain, and these neuronal oscillations are commonly referred to as brain waves (Buskila et al., 2019). When measuring the electrical activity of the brain using electroencephalography (EEG), different brain states are categorized based on distinct wavelength frequencies. Distinguishable brain states can be conceptualized as corresponding to varying degrees of alertness or arousal, and are further differentiated by their associated behavioral characteristics (Lee & Dan, 2012). Research has established that these ongoing fluctuations in state strongly influence how the brain responds to stimuli and makes behavioral decisions (Zagha & McCormick, 2014). Additionally, fluctuations in brain states are tightly coupled to variations in pupil diameter (Reimer et al., 2016). As such, pupillometry is a non-invasive technique used to index fluctuations in arousal state (McGinley et al., 2015).

Brain state patterns are often used to monitor and study the stages of sleep (Girardeau & Lopes-Dos-Santos, 2021). Sleep is understood to be composed of a series of stages that are defined by their EEG and electromyography (EMG) signatures (Figure 1), and a dynamic balance occurs between neural systems throughout the duration of the sleep-wake cycle (Stevner et al., 2019). Animals experience two primary phases of sleep, which are termed rapid eye

movement (REM) and non-rapid eye movement (NREM) (Patel et al., 2022). Each stage of sleep is characterized by variations of brain wave patterns, eye movement, and muscle tone (Patel et al., 2022). In mice, states are classified into Wake, NREM, and REM (Yamabe et al., 2019). The waking state is characterized by desynchronized EEG activity and high EMG power (Xu et al., 2015). During the NREM phase of sleep, the EEG reports synchronized activity with high power in the delta band (0.5-4 Hz) and low EMG activity (Xu et al., 2015). EEG recordings during the REM phase paradoxically resemble wakefulness, and the body's skeletal muscles are atonic except for those necessary for breathing and the characteristic rapid movement of the eyes (Jones, 1994). REM sleep is also characterized by increased power at theta (4-8 Hz) frequencies and a distinct spike in the ratio of theta to delta power, also referred to as T:D ratio (Xu et al., 2015). An additional brain state of relevance is one termed Quiet Wake, which is distinguished from Active Wake by behavioral inactivity. Research in human participants has shown that Quiet Wake facilitates the formation of insight, or the mental restructuring of previously acquired information, in a manner similar to sleep (Craig et al., 2018).

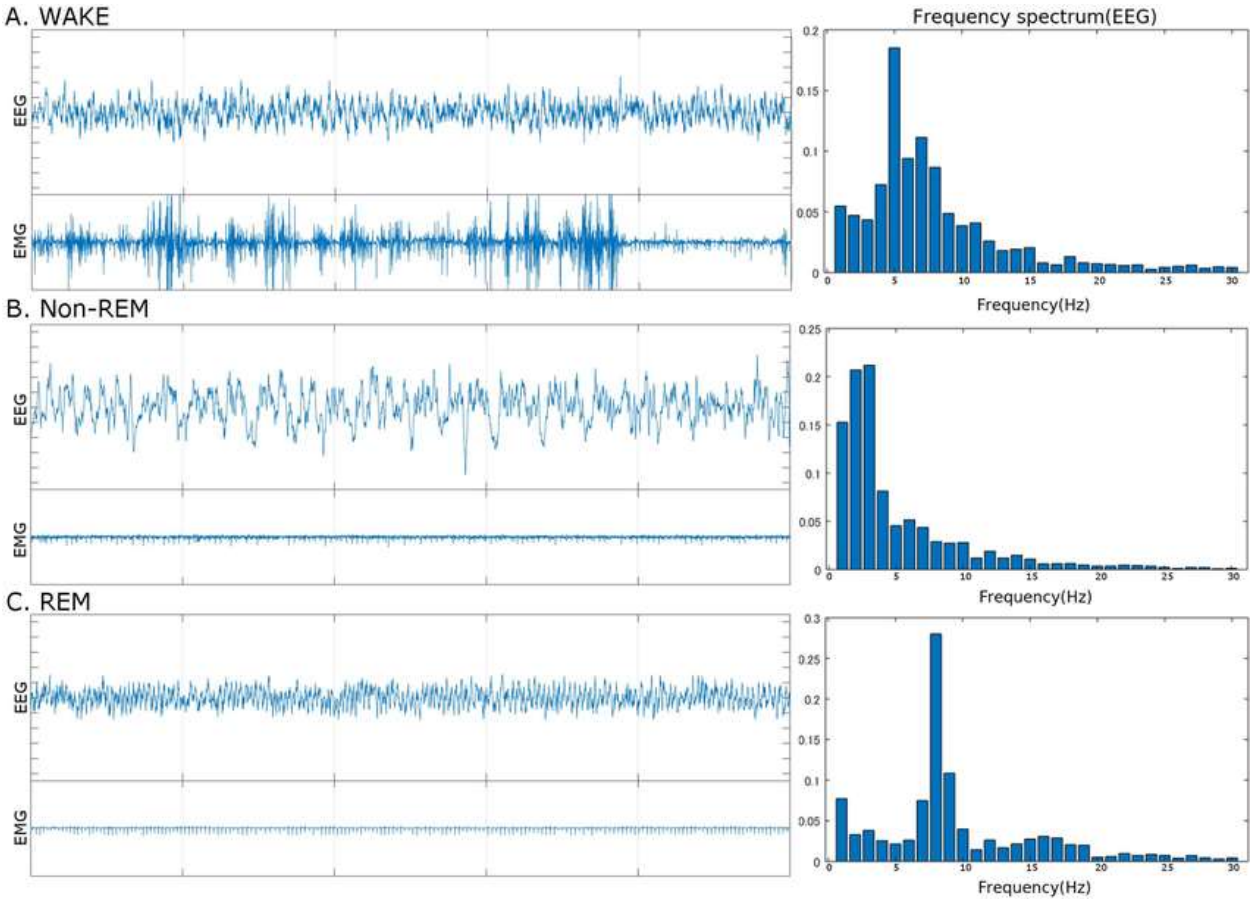


Figure 1: Example EEG and EMG signals for Wake, NREM, and REM states (Yamabe et al., 2019)

Typical samples of EEG and EMG recordings from mice classified into Wake (**A**), NREM (**B**), and REM (**C**) states. Additionally, includes typical EEG frequency spectra (power band spectra) to the right of EEG and EMG panels. Figure from Yamabe et al., 2019.

The dynamics of natural sleep states have been extensively researched (Hermans et al., 2022; Jones, 1994; Patel et al., 2022; Watson et al., 2016). Despite their ability to induce altered states of consciousness and neuronal activity that both parallel and diverge from those of endogenous brain states, far less is understood about the arousal states induced by psychedelics, such as 2,5-Dimethoxy-4-iodoamphetamine (DOI) (Doss et al., 2021; Tagliazucchi et al., 2014). The term "psychedelic" was first coined by psychiatrist Humphry Osmond in 1956, which he derived from the Greek words "psyche "and "dēlos" such that its composite meaning is "mind

manifesting" (Calvey & Howells, 2018). The very etymology of the term "psychedelic" implies that these substances can reveal the hidden potentials of the mind, foreshadowing their renaissant application to the study of consciousness in recent years following decades of limited research due to legal restrictions (Calvey & Howells, 2018; Maćkowiak, 2023). Psychedelics have been found to cause prompt and enduring behavioral plasticity in studies of both humans and mice (Calder & Hassler, 2023; Nardou et al., 2023). DOI is an agonist of 5-HT2A serotonergic receptors, and the documented effects of psychedelics at these receptors include increasing neuroplasticity, re-opening critical periods for social reward learning, and alleviating the symptoms of neuropsychiatric disorders like obsessive compulsive and post-traumatic stress disorders (Gray & Roth, 2001; van Elk & Yaden, 2022; Wallach et al., 2023).

DOI has recently been found to consistently elicit ~0.03 Hz infra-slow pupil oscillations (Figure 2; Vickers, 2025) which strikingly parallel the infra-slow oscillatory activity known to occur during NREM sleep (Lázár et al., 2019; Lecci et al., 2017; Watson, 2018). These infra-slow oscillations are distinctive as they are rarely observed in waking states, though their consistent presence following DOI administration provides an opportunity to investigate how the pupillary dynamics and corresponding cortical activity of psychedelic states overlap or deviate from those of natural brain states (Kropoptov, 2022; Xiang et al., 2023). Additionally, serotonergic psychedelics have recently been found to induce sleep-like spectral signatures in hippocampal and prefrontal cortical local field potential (LFP) recordings, and this psychedelic-induced sleep-like state during wakefulness has previously been described as "paradoxical wakefulness" (Bréant et al., 2022; Souza et al., 2024; Thomas et al., 2022). Given this distinct parallel between the DOI and NREM states, as well as the established use of electrophysiology to compare psychedelic and sleep states, there is a compelling need to more closely examine the

extent to which the DOI-induced arousal state resembles or diverges from naturally occurring (non-psychedelic induced) brain states. Comparing and contrasting the multimodal features of these states is essential to determine whether psychedelic-induced states are fundamentally distinct from -- or a pharmacologically altered version of -- endogenous brain states.

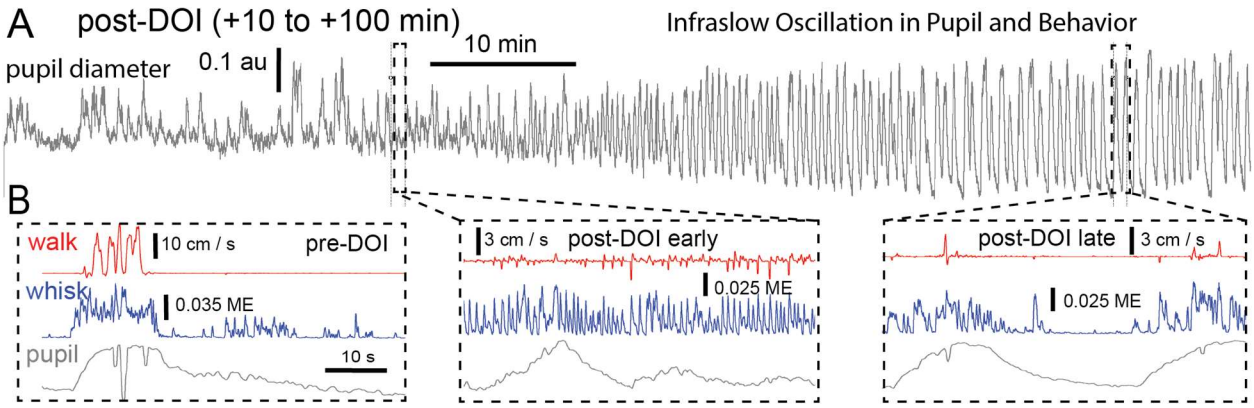


Figure 2: DOI induces a pronounced infra-slow oscillation in pupil diameter and behavioral state (Vickers, 2025)

(**A**) Continuous trace of pupil diameter from 10 to 100 minutes after subcutaneous injection of DOI (10 mg/kg). Note the appearance of a highly regular infra-slow oscillation of about once per minute in pupil diameter. This effect lasts for 2+ hours. (**B**) Prior to SC (subcutaneous) injection of DOI, spontaneous behavior, particularly whisker movements and pupil diameter, can exhibit a few cycles of dilation/constriction in the resting state, but these are typically irregular and intermixed with bouts of walking/whisking. For approximately 5-40 minutes following the IP injection of DOI, the mouse exhibits a prominent 1 Hz whisker twitching behavior that is relatively independent of ongoing large fluctuations in pupil diameter and not associated with running. After approximately 30-40 minutes, and for up to 2 hours or more, this 1 Hz whisker twitching behavior becomes a prominent, highly regular and coordinated infra-slow oscillation of pupil diameter, whisker movements, and walking. Courtesy of Evan Vickers, McCormick Lab.

Swift variations in brain state are governed by various neuromodulatory networks (Lee & Dan, 2012; McCormick et al., 2020). One such network is that of noradrenaline (NA), also known as norepinephrine (NE), which is a neurotransmitter involved in the regulation of attention, arousal, and general stress reactions (Berridge, 2008; Poe et al., 2023). As illustrated in

Figure 3, the neurons of the noradrenergic system in the brain primarily originate in the locus coeruleus, a nucleus located deep in the pons of the brainstem, and sends axonal projections across the brain including to the thalamus and cortex (Koshmanova et al., 2023; Poe et al., 2023). Fluctuations in the activity of the locus coeruleus-noradrenaline (LC-NA) system are closely correlated with changes in pupil diameter, and pupil dynamics have been previously used as a proxy for noradrenergic tone (Joshi et al., 2016; Maheu et al., 2025; Reimer et al., 2016; Turner et al., 2023; Weiss et al., 2025). It has also been found that LC-NA neurons phase-lock to the infra-slow cortical oscillation observed during NREM sleep, and that infra-slow LC-NA activity serves as one of the "gatekeepers" of transitions between NREM and REM sleep states (Xiang et al., 2023; Osorio-Forero et al., 2025). LC-NA activity during sleep interferes with NREM delta power and sleep spindles, as well as REM theta power (Swift et al, 2018).

Previous work demonstrates that power in the sigma band (10-16 Hz), which is particularly prominent during NREM infra-slow oscillatory activity and closely correlated to sleep spindles, is anticorrelated to noradrenergic axon activity (Osorio-Forero et al., 2021; Osorio-Forero et al., 2025). Increased sigma power is associated with reduced noradrenergic tone, which is reflected in pupil constriction. Given these established relationships between LC-NA activity and both pupil dynamics and NREM infra-slow oscillations, it has been proposed that the noradrenergic system may play a primary role in generating and modulating the ~0.03 Hz infra-slow pupil oscillation consistently observed following the administration of DOI (Vickers, 2025). Although DOI primarily acts on 5-HT2A receptors, the noradrenergic and serotonergic systems are known to interact extensively (Blier, 2001; López-Rubalcava & Fernández-Guasti, 1994; Pape & McCormick, 1989). As such, investigating how DOI affects LC-NA activity, specifically regarding the infra-slow pupil oscillation, will provide insight into

the neuromodulatory mechanisms underlying psychedelic-induced states of arousal and how they relate to endogenous states like NREM.

To record the activity of axons during ongoing behavior, researchers employ a technique known as *in vivo* calcium imaging (see Figure 4). Calcium imaging reliably indicates activity in neurons because the underlying cellular mechanisms of this activity include a rapid influx of calcium ions into the neuron after firing (Smetters et al., 1999). The neurons of animals with genetically encoded calcium indicators (GECIs) report the presence of calcium using fluorescent proteins, such that when an axon is active it can be seen as increased fluorescence emission (Stosiek et al., 2003). A mesoscope -- a type of two-photon microscope with a high spatial resolution and large field of view -- is used to image the animal's cortex through an implanted cranial window so that researchers can record the neural activity in the region of interest (Stosiek et al., 2003; Sofroniew, 2017). The mesoscope allows for the simultaneous measurement of the activity between individual neurons or their axons, which is crucial to studying the dynamics of neural circuitry like that of the noradrenergic system (Sofroniew, 2017).

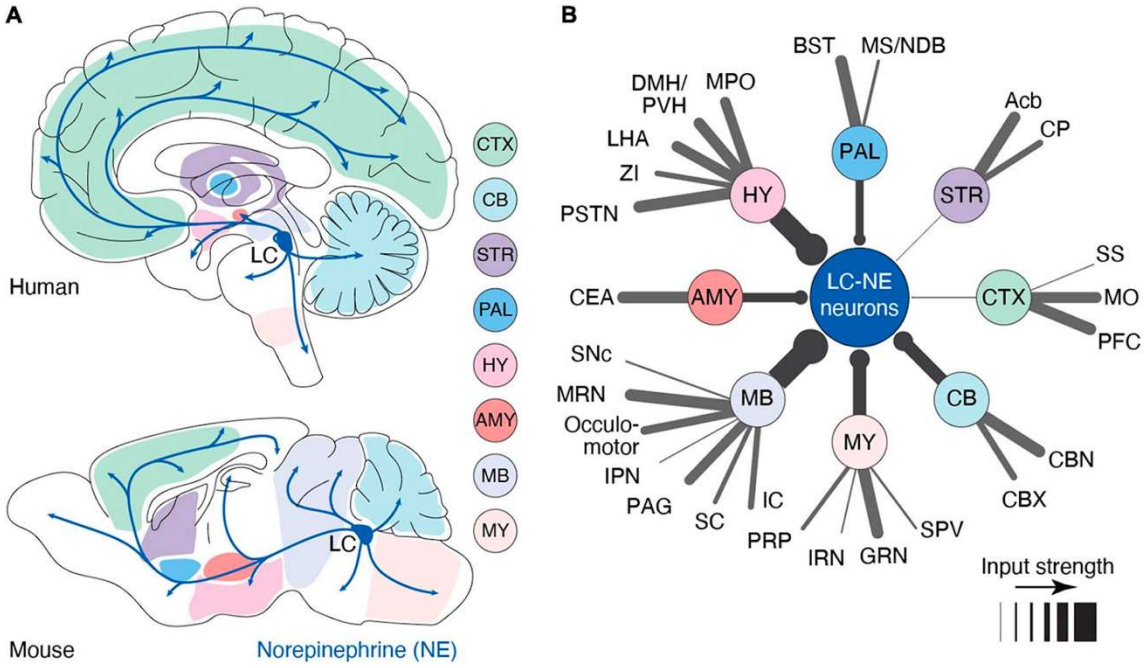


Figure 3: Anatomical diagrams of the locus coeruleus and its connections in the human and mouse brains (Breton-Provencher et al., 2021)

(**A**) shows diagrams of the anatomy of LC-NA projections in both the human and mouse brains. Shaded regions show areas thought to send input to LC. (**B**) demonstrates distal inputs to LC-NA system with primary inputs in colored circles (cortex = CTX; striatum = STR; pallidum = PAL; hypothalamus = HY; amygdala = AMY; midbrain = MB; medulla = MY; cerebellum = CB) connected to secondary inputs via lines whose thickness represents varying input strengths (motor area = MO; somatosensory area = SS; nucleus accumbens = Acb; caudoputamen = CP; bed nucleus of stria terminalis = BST; medial septal/diagonal band nucleus = MS/NDB; dorsomedial/paraventricular nucleus = DMH/PVH; lateral hypothalamic area = LHA; zona incerta = ZI; parasubthalamic nucleus = PSTN; central amygdala = CEA; substantia nigra = SNc; midbrain redicular nucleus = MRN; interpeduncular nucleus = IPN; periaqueductal gray = PAG; super colliculus = SC; inferior colliculus = IC; nucleus prepositus = PRP; intermediate reticular nucleus = IRN; gigantocellular reticular nucleus = GRN; spinal nucleus of the trigeminal = SPV; cerebellar cortex = CBX; cerebellar nuclei = CBN). Figure from Breton-Provencher et al., 2021.

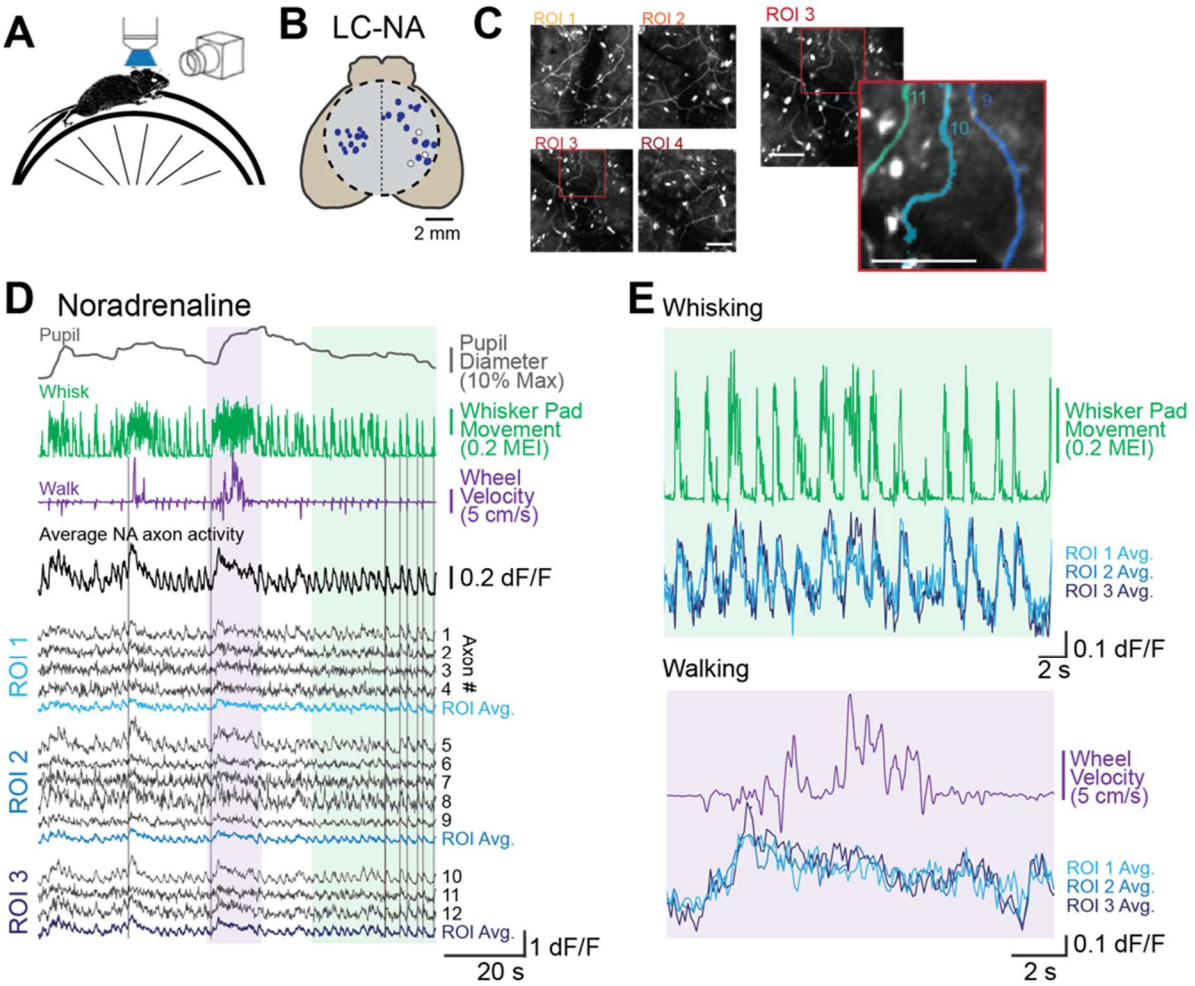


Figure 4: Two-photon imaging of dorsal cortical noradrenergic activity (Collins et al., 2023)

(**A**) Schematic of experimental setup. Awake mice were placed atop a running wheel underneath a two-photon mesoscope objective for imaging of axonal activity through GCaMP6s. A side camera was used to capture facial movements. (**B**) To allow for imaging across a large region of cortex, mice were implanted with a glass cranial window (dotted circle) on the dorsal brain surface. Recordings could be collected from regions of interest (ROIs) within a 5 × 5 mm field of view. Estimated locations of all ROIs are shown for LC-NA axon segment recordings. Size of each circle corresponds to the size of the corresponding square ROI. White circles represent ROIs shown in panels (**D–E**). (**C**) Left: mean projection image of four simultaneously recorded ROIs. Right: example of Suite2P-defined axons. Three axons are shown in the inset image, which correspond to the three blue dF/F traces in panel (**D**). Scale bars represent 50 μm. (**D**) Example recordings of GCaMP6s activity in 13 LC-NA simultaneously imaged axon segments in three ROIs. (**E)** Pupil diameter, whisker pad movement, and wheel movement (both rotational and vertical) are shown alongside dF/F of individual axons recorded simultaneously across ROIs shown in panel (**B**). Average activity across all axons simultaneously monitored as well as within a ROI are shown (**D**). Colored regions in (**D**) are expanded for illustration in (**E**). Axon GCaMP6s data in (**E**) represented as ROI averages. Histological investigation revealed that GCaMP6s expression was specific for noradrenergic neurons and axons. Figure adapted from Collins et al., 2023.

Mice are used as a model organism with the purpose of researching neural processes that are shared across animal species (Osuchowski et al., 2014). Animals are used in research because they are the most comprehensive model of the complex functions of a whole-organ system, such as the brain and body, and experiments can be performed that are not possible in humans (Chang & Grieder, 2024; Osuchowski et al., 2014). An animal model may not be used in research if the proposed experiment can be effectively carried out with an alternative model, such as cell and tissue cultures or computer simulations (Gross & Tolba, 2015). The most obvious beneficiaries of animal research are those treated for previously incurable diseases, although virtually everyone alive today has benefited in some way or another (Gross & Tolba, 2015). This includes vaccines, antibiotics, antidepressants, surgical procedures, and myriad other treatments developed and tested in animals (National Academy of Sciences, 1991). More than two thirds of the research awarded the Nobel Prize in physiology or medicine has directly involved animal

models (National Academy of Sciences, 1991). The humane care of laboratory animals is both ethically and scientifically imperative to animal research, which has and continues to immensely benefit the scientific field (Gross & Tolba, 2015; Osuchowski et al., 2014). All experiments are carried out under the scrutiny and approval of the University of Oregon's Institutional Animal Care and Use Committee (IACUC). This committee must have at least five members including a veterinarian, a practicing scientist with animal research experience, a member whose concerns lie in a non-scientific discipline, and an individual unaffiliated with the institution (*Animal Welfare Services | Research and Innovation*).

In this study, we aim to investigate the neural and behavioral effects of the serotonergic psychedelic DOI with a particular focus on how measurable features of the brain state that it induces relate to the established features of endogenous wake and sleep states. In Phase 1, we validate the feasibility of studying sleep dynamics in a head-fixed recording paradigm. During Phase 2, we employ electrophysiological and behavioral metrics typically used to distinguish endogenous arousal states (Active Wake, Quiet Wake, NREM, and REM) in order to assess how the state induced by DOI compares to these canonical brain states. Finally, Phase 3 explores how DOI affects noradrenergic activity and interrogates the potential role of noradrenaline in the modulation of the characteristic DOI infra-slow pupil oscillations. Ultimately, this project seeks to evaluate how the DOI-induced state resembles or diverges from natural states of arousal, contributing to our collective understanding of how psychedelics interact with the fundamental neuromodulatory systems governing brain arousal and plasticity.

# Methods

## Animals

All experimental procedures were approved by the Institutional Animal Care and Use Committee (IACUC) at the University of Oregon and were carried out in accordance with the National Institute of Health Guide for the Care and Use of Laboratory Animals. A total of 4 (N = 4) mice were used throughout the three phases of this study. Mice were singly housed with ad-libitum access to food and water. Enrichment included arc houses, crinkle paper, and toilet paper rolls. They were housed in a 10-hour dark/14-hour light cycle room so that their sleep schedules aligned with the operating hours of the lab (lights on between 06:00 and 20:00).

Table 1: Demographics of animals used in study

| Mouse ID | 102 | 103 | 111 | 112 |
|---|---|---|---|---|
| Genotype | DBH-Ai162 | DBH-Ai162 | DBH-Ai162 | DBH-Ai162 |
| Sex | F | M | M | F |
| Date of birth | 07/01/24 | 06/04/24 | 7/15/2024 | 5/12/2024 |
| Date of implant | 09/19/24 | 09/20/24 | 1/17/2025 | 3/17/2025 |
| Phase of study | 1 | 1, 2 | 3 | 2 |

## Surgeries

All surgical procedures were performed in an aseptic environment. Mice were initially anesthetized at 4% isoflurane and then an appropriate depth of anesthesia was maintained under 1-2% isoflurane at an oxygen flow rate of 1.5 L/min. Once sedated, analgesic injections were given to mediate pain and inflammation (Buprenorphine SR, 0.5 mg/kg; Meloxicam SR, 6 mg/kg). The animals' body temperature was monitored and maintained at 36.5 degrees Celsius using a heating pad. After removing the overlying skin and connective tissue, a titanium

headpost was affixed to the skull with dental cement. Small craniotomies for the iEEG electrodes were drilled over the primary motor cortex and cerebellum, and an EMG electrode was immobilized in the dorsal neck muscles. Custom electrodes for iEEG recordings were made from silver wire (0.010'', A-M Systems) and soldered to an insulated lead. For EMG recordings, electrodes were fabricated from teflon-coated silver wire (0.015'', A-M Systems). After being implanted, the electrodes and headpost were covered with transparent dental acrylic. Once the acrylic was sufficiently dried, the mouse was taken off anesthesia and left to recover in a clean cage in a thermo-regulated recovery chamber. Post-operative care included the administration of subcutaneous lactated ringer's solution as needed for 1-3 days, and recordings started after a minimum of three additional days of recovery.

**Handling and Sleep Training**

Data acquisition was not initiated until the mice had at least three days of post-operative recovery. Throughout the recovery period, mice were habituated to gentle handling for at least three consecutive days. They were habituated to the behavior rig via three successive days of head-fixation, beginning with 15 minutes of head fixation and increasing by increments of 15 minutes in the following days (Day 1 = 15 minutes, Day 2 = 30, Day 3 = 45). A flexible head-fixation post was used to keep the animal's head at a 30-degree angle with their nose down to imitate their natural sleeping position (Figure 5). The behavior room and satellite room where the mice were housed were both maintained at a comfortable temperature and level of noise, and mice cages were covered to limit exposure to external stimuli during any transportation between rooms. Mice were held in a sound and light isolated Faraday cage during habituation and recordings, and they were continuously monitored via infrared camera and light. It should be

noted that mice cannot see infrared light, so the light would not disturb their sleep (Warren, 2019).

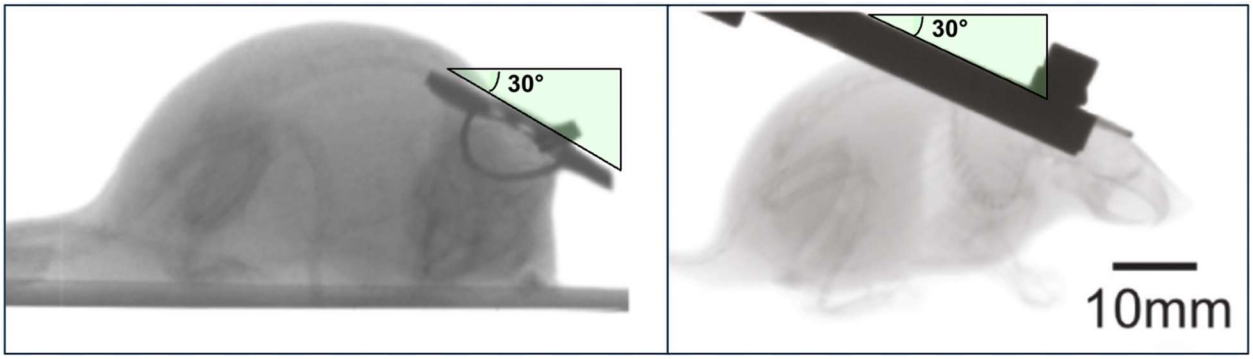


Figure 5: X-rays of mouse sleeping position (Yüzgeç et al., 2018)

**Left**: X-ray of freely moving mouse natural sleeping position shows 30-degree angle (nose down) of head. **Right**: 30-degree angle achieved in head-fixed recording paradigm. Adapted from Yüzgeç et al., 2018

*Data Acquisition*

**Electrophysiology**

EMG and iEEG signals were acquired at 1kHz using AM-Systems amplifiers (AC/DC Differential Amplifier) and digitized through a Power1401 data acquisition interface (Cambridge Electronic Design, Power1401). The digital waveform traces were displayed and recorded in Spike2 (Version 8) alongside the whisk, walk, and pupil metrics.

**Pupil, Walk, and Whisk Metrics**

Pupil diameter was measured simultaneously in real time and offline using a custom LabVIEW script. Walking speed was measured via rotary encoder (McMaster-Carr) attached to the wheel (see Figure 6). The wheel was supported by springs and the rotary encoder also detected vertical movements of the wheel, which could occur with or without walking. To measure whisking movement, a region of interest (ROI) was delineated over the whisker pad and

the motion energy index (MEI) was calculated across the video, where MEI was the sum of the absolute change in the pixel intensity within the ROI between adjacent video frames (Collins et al., 2023).

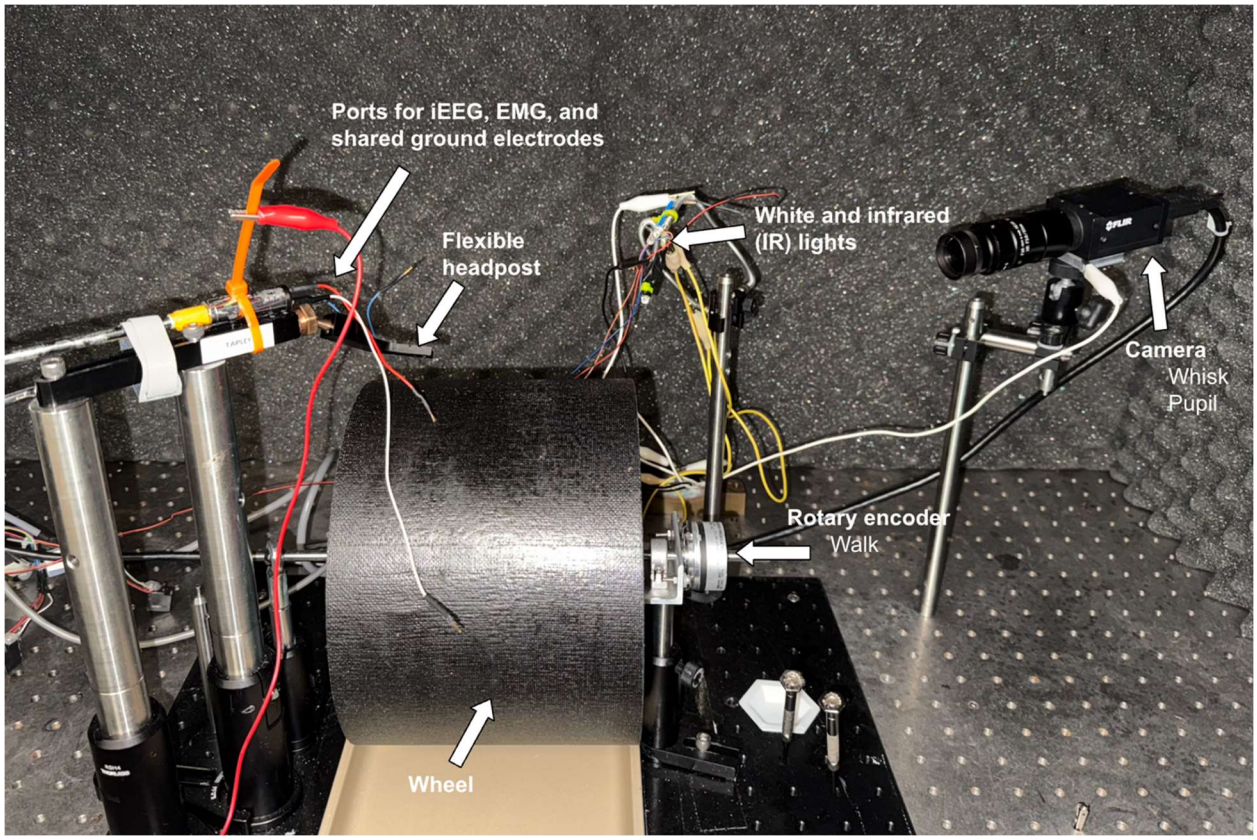


Figure 6: Diagram of experimental setup

Image of behavior rig (Faraday cage) with various parts labeled, including wheel, rotary encoder (for walk data acquisition), camera (for acquisition of both whisk and pupil metrics), flexible headpost support arm (Vickers & McCormick, 2024) to facilitate 30-degree angle of head to mimic natural sleeping position, ports to connect electrodes to amplifiers for iEEG and EMG recordings, and white and infrared lights to optimize illumination of the pupil. Unlabeled parts of note include alligator clips used for grounding, tray to aid maintenance of a clean experimental environment, and tools to secure headpost during head-fixed recordings.

## DOI Administration

Powdered DOI (0.4 mg/mL) was diluted in a sterile saline solution with 0.2 μm filtration. The dilution was transferred to Eppendorf tubes from the sterilized glassware it was prepared in and stored at -20 degrees Celsius for up to 6 months prior to the time of delivery. DOI was delivered by subcutaneous injection (10 mg/kg, each injection dosed at 5 mL/g of body weight, 1 mL syringe, 23 G needle) after at least 30 minutes of baseline data acquisition during phases 2 and 3 of this study.

## Two-Photon Imaging

DBH-cre mice expressing cre-recombinase in noradrenergic neurons were crossed with Ai162 mice cre-dependently expressing GCaMP6s to assess noradrenergic activity with calcium imaging (IMSR Cat# JAX:033951, RRID:IMSR_JAX:033951; ISMR Cat# JAX:031562, RRID:ISMR_JAX:031562). It has been histologically verified that mice from the DBH-Ai162 line used in this study reliably express GCaMP6s in noradrenergic axons (Figure 7). Two-photon imaging of DBH-Ai162 mice was carried out using a ThorLabs Multiphoton Mesoscope with a 12 kHz Resonant Scanner, Virtually Conjugated Galvo Scanner Set, and 1 mm range Remote Focusing Unit to allow for swift imaging across various ROIs with unique X, Y, and Z coordinates (Collins et al., 2023; Sofroniew et al., 2016). A Ti-sapphire laser tuned to 920 nm was used to excite GCaMP6s (MaiTai, Spectra Physics), and the Scan Image software Vidrio was used for imaging. A minimum resolution of 1 μm per pixel was used to image axonal processes at a frequency of 5-10 Hz with a field of view of 300 x 300 μm to optimize imaging based on the established kinetics of GCaMP6s (Chen et al., 2013; Collins et al., 2023).

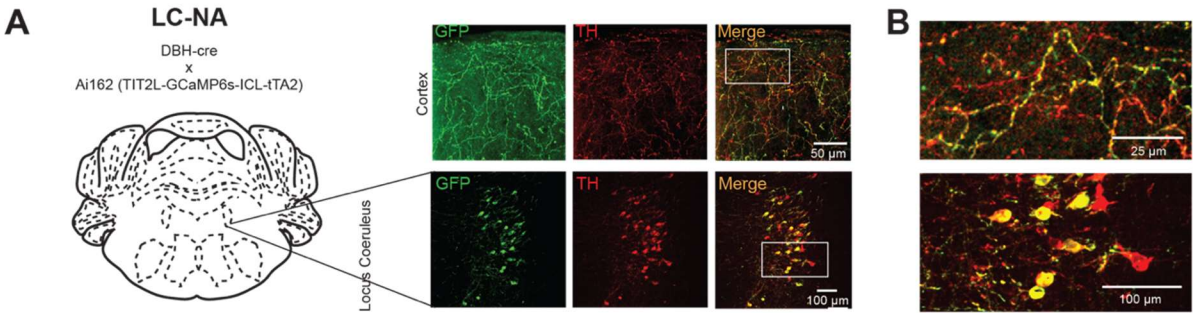


Figure 7: Histological verification of DBH cre X Ai162 mice (Collins et al., 2023)

(**A)** Histological verification of DBH cre X Ai162 mice demonstrating that locus coeruleus neurons and axons in the cerebral cortex that are labeled with GFP (GCaMP6s) are also immunopositive for tyrosine hydroxylase (TH+) and therefore are noradrenergic. The vast majority of cells immunopositive for GFP in the locus coeruleus are also immunopositive for TH (n=559/584 neurons; 96%; N=2 mice). (**B)** Expansion of axons and cells in C for clarity. From Collins et al. 2023.

*Data Analysis*

**Manual Sleep State Classification**

Recording sessions from Phase 1 were sleep scored in Spike2 using a CED script for manual sleep staging and event marking (Cambridge Electronic Design, sleepscore706s2s). The raw iEEG and EMG traces were processed for sleep state classification in several consecutive steps. First, a notch resonator filter was applied to remove 60 Hz noise. This was followed by a Butterworth bandpass second order filter (0.1 to 30 Hz for iEEG, 30 to 300 Hz for EMG), and then spectral analysis of the iEEG signal was carried out via Fast Fourier Transform (FFT). The duration of the recording session was divided into 5 second epochs which were manually assigned a state label based on the EMG tone, iEEG power bands, and theta:delta ratio (See Table 2). Epochs were classified as REM when the Theta:Delta ratio was at least 2 standard deviations above its mean and EMG power was 2 SD smaller than its mean (similar to Yüzgeç et al., 2018). Active Wake was distinguished from Quiet Wake by its high EMG power, and NREM was identified by its characteristic high-amplitude, synchronized slow-wave iEEG activity and low EMG power (per Xu et al., 2015).

Table 2: Criteria for sleep state classification from frontal iEEG and nuchal EMG electrode recordings

| State | iEEG | EMG | Power bands | Theta:Delta ratio |
|---|---|---|---|---|
| Active Wake (AW) | High-frequency desynchronized activity with low amplitude | High muscle tone | Mixed activity | Low |
| Quiet Wake (QW) | Higher amplitude, slower oscillations, still high frequency and desynchronized | Moderate muscle tone | Mixed activity, possibly a higher delta than active wake | More balanced, theta slightly higher than delta in some cases |
| NREM Sleep (NREM) | Dominated by synchronized slow-wave oscillations (delta waves), sonogram will show low-frequency activity and high amplitude, manual ID of k-complexes/sleep spindles | Low muscle tone | High delta power | Very low, dominated by delta |
| REM Sleep (REM) | Mixed frequency desynchronized activity (low amplitude, high-frequency oscillations), sonogram may show bursts of activity but with lower frequency | Very low muscle tone, EMG often shows little to no activity (atonia) | Elevated theta power relative to delta | High, theta dominates |
| Uncertain | This state was used when the signals didn't clearly match any of the above criteria, or if the data quality was too poor to make a definitive classification. | | | |

**DOI**

To evaluate how the state of arousal induced by DOI compared electrophysiologically and behaviorally to endogenous states, DOI recording sessions were blind-scored using the same multimodal criteria as was utilized to sleep-score control sessions into epochs of Active Wake, Quiet Wake, NREM Sleep, and REM Sleep (AW, QW, NREM, and REM, respectively). Infra-slow (0.01 to 0.1 Hz) pupil oscillations were manually identified after scoring from the DOI sessions and during NREM epochs from the control sessions. Power in the sigma band was extracted from the iEEG signal by applying a bandpass filter from 10-16 Hz. Figures comparing the electrophysiological and behavioral data from control and DOI recordings were generated using custom Python scripts and Adobe Illustrator.

**Calcium Imaging**

Calcium imaging data were analyzed following previously described methods (Collins et al., 2023; Francis, 2021; Nelson & Mooney, 2016; Reimer et al., 2016). Axons were identified from 2-photon mesoscopic imaging data using Suite2p (Pachitariu et al., 2017). Axon segments expressing GCaMP6s (DBH-Cre x Ai162 mice) were imaged in 6 ROIs (300 x 300 μm, 2 pixels/μm) identified across the dorsal cortex and imaged at ~5-10 Hz with 920 nm excitation wavelength. For detailed methods, see Collins et al., 2023. To summarize: All axon segments identified by Suite-2P were manually verified by confirming that a significant length (~20 μm) of the axon segment was within the ROI. Any identified region that did not correspond to a clearly identifiable axonal process was excluded. Axon segments that were identified by Suite2P as distinct from one another but visually determined to be part of the same axonal process -- e.g. there was clear continuity of the axon form connecting the segments together -- were also

excluded. Motion control was achieved by using autofluorescent ‘blebs’, which are imaged alongside axons but do not exhibit calcium-dependent activity, as controls to account for movement, and Suite2P also carries out rigid and non-rigid motion correction (Collins et al., 2023). Calcium fluorescence data traces were pre-processed by up-sampling to 100 Hz and low-pass filtering to 10 Hz. Signal-to-noise ratios for each trace were calculated by dividing max power within the frequency range of 0.05 and 0.5 Hz by the mean power between the frequency range of 1 and 3 Hz. Traces with a signal-to-noise ratio less than log(20) were excluded from further analysis. $\Delta F/F$, a measure of change in fluorescence over baseline fluorescence, was calculated as the primary metric to quantify changes in fluorescent axonal activity. Baseline fluorescence was defined as the median fluorescence value for each session. To correct for possible contamination of the axonal fluorescent signal by the fluorescent activity of surrounding neuropil (network of neuronal processes), the fluorescent signal from the full ROI was averaged and this neuropil signal was subtracted from the axonal fluorescence signal.

# Results

## Phase 1: Head-Fixed Mice Exhibit Natural Sleep States

### *Sleep State Identification Using iEEG and EMG*

To validate that mice could reliably engage in natural sleep in a head-fixed paradigm (as previously described in Yüzgeç et al., 2018), recording sessions containing iEEG, EMG, whisk, walk, and pupillometry data were classified using conventional sleep scoring guidelines with identifiable spectral and behavioral features. REM sleep was characterized by an acute increase in the Theta:Delta power ratio and sustained EMG atonia (Figures 8 & 9). These features were reliably observed across recording sessions, aligning with the previously established characteristics of the REM state. Pupillary dynamics consistent with rapid eye movements provided additional behavioral validation (Figure 9).

iEEG and EMG signals across different states within recording sessions demonstrate the electrophysiological distinctiveness of REM, NREM, AW, and QW states. As illustrated in both Figures 8 and 9, NREM exhibited elevated power in the delta band and a more moderate suppression of muscle tone compared to REM. AW showed mixed frequency, highly variable iEEG activity and elevated EMG tone during periods of behavioral activity, whereas QW exhibited similar spectral patterns during epochs of behavioral inactivity with more moderate EMG tone (Figure 10).

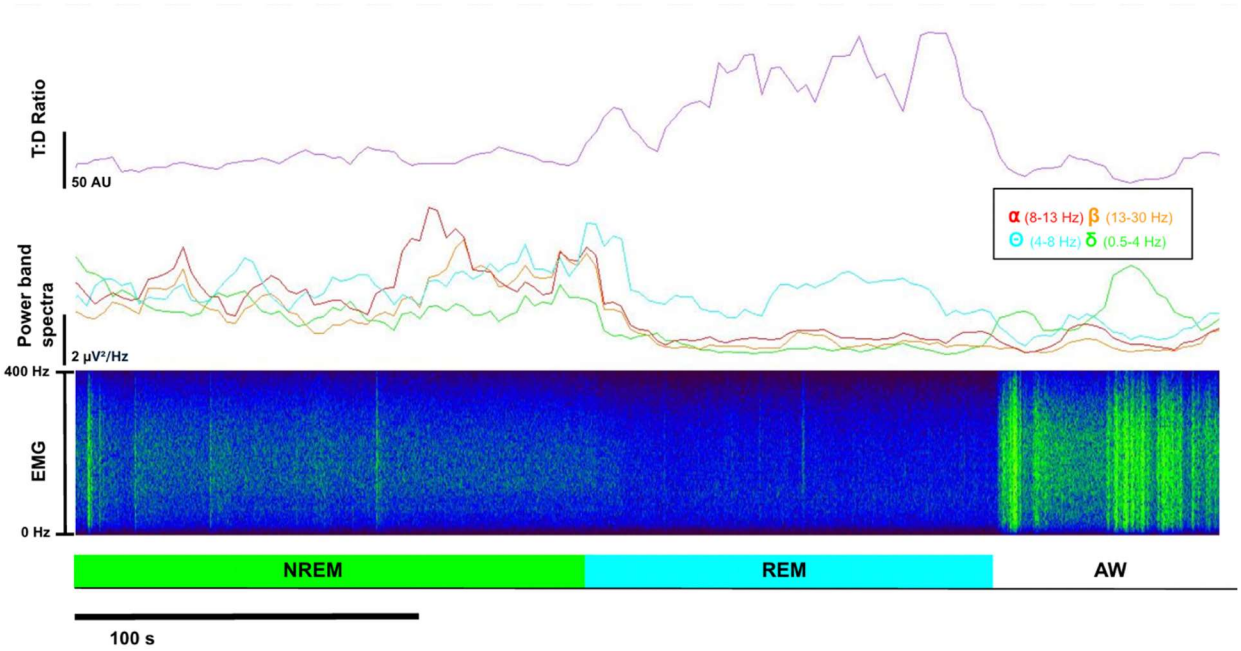


Figure 8: REM Sleep Episode Nestled Between Epochs of NREM and AW with EMG, Spectral Power Bands, and T:D Ratio

A representative example of REM sleep recorded from a head-fixed mouse with characteristic behavioral and electrophysiological markers. From bottom to top, plot shows state labels for 5 second epochs (NREM = light green, REM = light blue, Active Wake = white), EMG sonogram, power band spectra (blue = theta, light green = delta, orange = beta, red = alpha), and T:D ratio (purple) across a 300 second period of a recording session. EMG sonogram during REM demonstrates signature atonia and power band spectra trace illustrates characteristic drop in delta power.

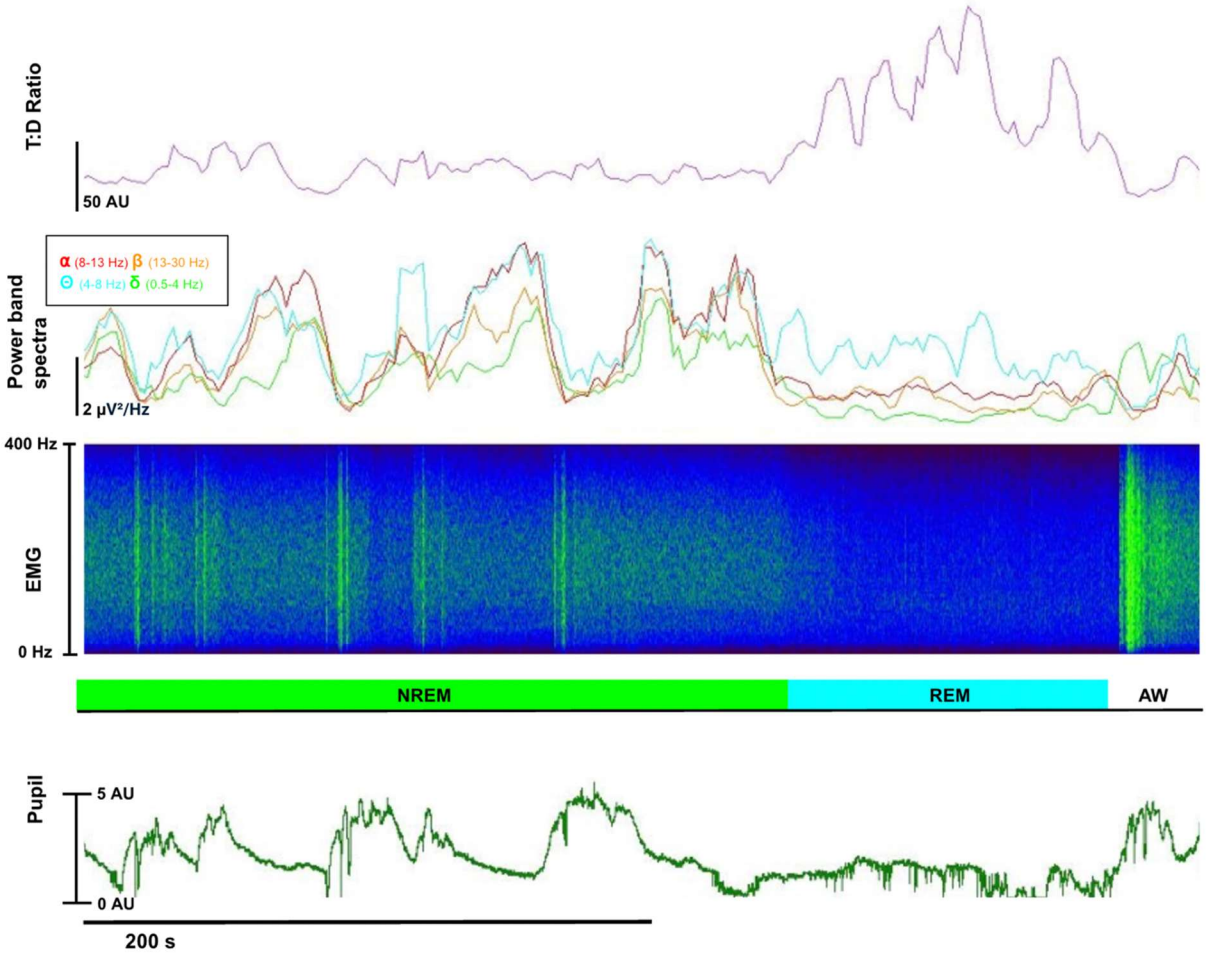


Figure 9: Comparison of REM and NREM with EMG, Pupillometry, Spectral Power Bands, and T:D Ratio

400 second snapshot of pupil diameter (dark green), state labels for 5 second epochs (NREM = light green, REM = light blue, Active Wake = white), EMG sonogram, power band spectra (blue = theta, light green = delta, orange = beta, red = alpha), and T:D ratio (purple) from recording session in head-fixed mouse. Note increase in T:D ratio at onset of REM from NREM coupled with sustained muscle atonia and decreased delta activity. Pupil trace shows high amplitude, infra-slow oscillatory pupil dynamics during NREM compared to smaller amplitude, higher frequency pupil movements during REM which return to baseline upon arousal (entering AW from REM).

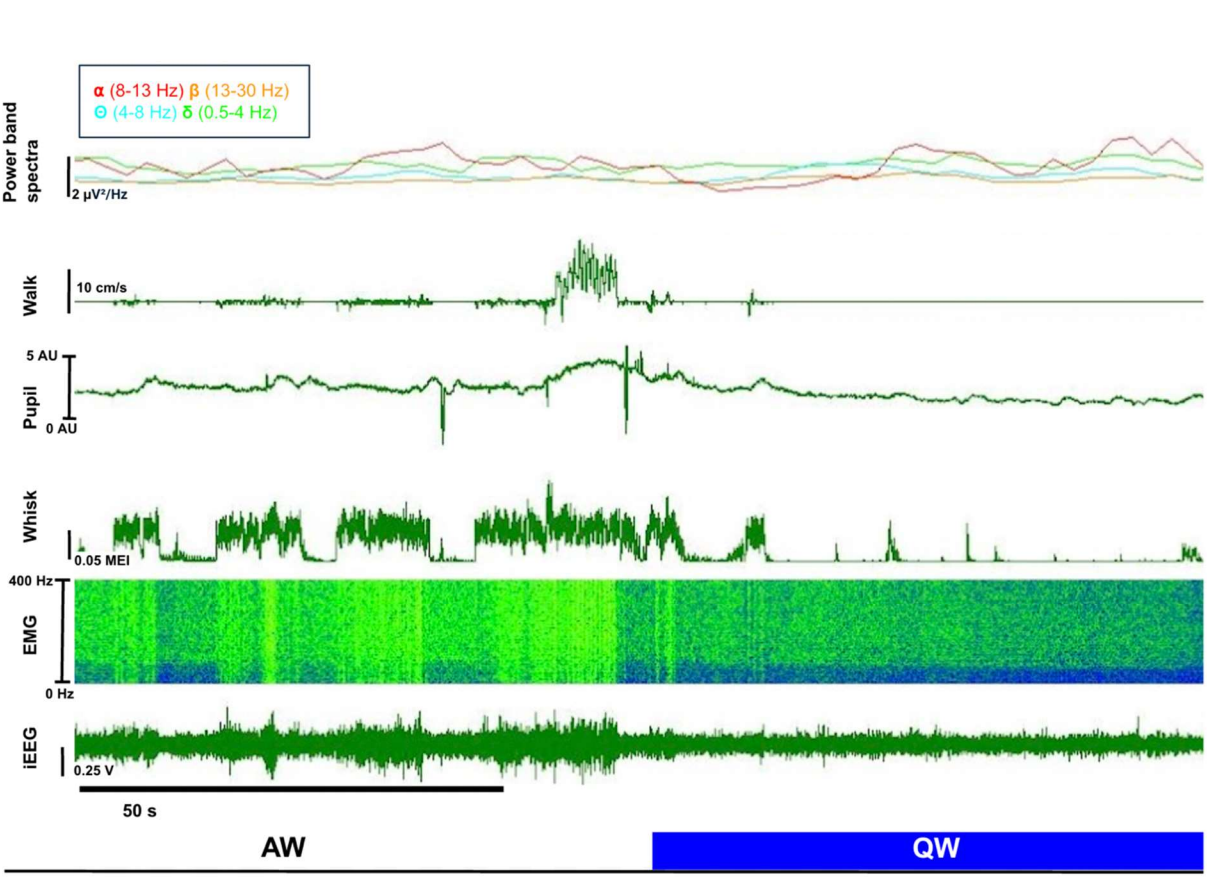


Figure 10: Active Wake vs Quiet Wake States with iEEG, EMG, Whisk, Pupil, Walk, and Power Spectral Band Traces

From top to bottom, shows power spectral bands (red = alpha, orange = beta, light green = delta, light blue = theta), 5 second state epochs (AW = white, QW = dark blue), Walk, Pupil, Whisk, EMG Sonogram, and iEEG traces. Behavioral metrics Walk and Whisk exhibit activity during AW and inactivity during QW. Moderate decrease in muscle tone from AW to QW visualized via EMG sonogram.

*Sleep Architecture in Head-Fixed Paradigm*

We observed full sleep cycles with transitions between AW, QW, REM, and NREM states in the head-fixed recording paradigm. These transitions between states were accompanied by predictable changes in the power spectra, EMG tone, and pupil diameter as illustrated in a representative recording session (Figure 11). These features were preserved across recording sessions, and state transitions were also reflected in the behavioral metrics. For example, pupil diameter consistently decreased while transitioning from wake to sleep states and returned to its baseline upon arousal from sleep. Multimodal data across representative sessions support the integrity of sleep architecture in head-fixed mice, demonstrating state-dependent changes in iEEG and EMG signals alongside corresponding fluctuations in walk, whisk, and pupil activity (Figures 11 & 12). Altogether, these data suggest that mice reliably transition between natural states of arousal under the head-fixed paradigm.

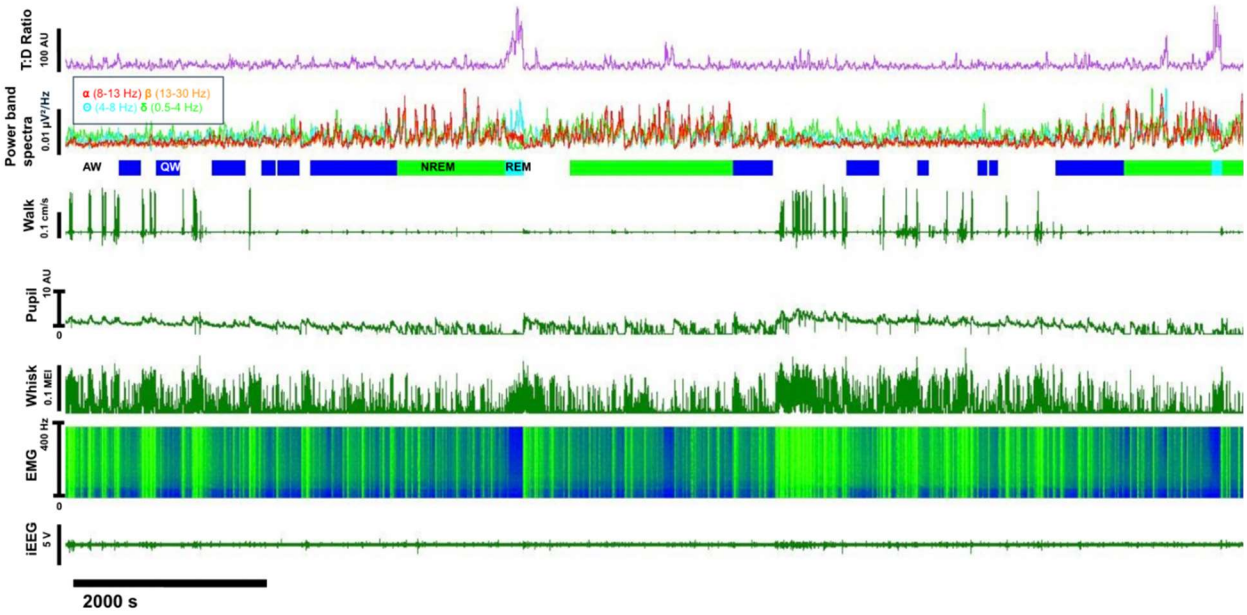


Figure 11: Representative Recording Session 1 with Overlapping Spectral Power Bands

Starting from the bottom, channels display data from iEEG, EMG Sonogram, Whisk, Pupil, Walk, state epoch (AW = white, QW = dark blue, NREM = light green, REM = light blue), power band spectra (red = alpha, orange = beta, light green = delta, light blue = theta) and T:D Ratio (purple). Shows electrophysiological signatures across arousal states and corresponding behavioral metrics, including acute rise in T:D ratio and EMG atonia during REM, Walk activity vs inactivity and associated muscle tone in AW vs QW, Pupil infra-slow oscillations during NREM. Consistently exhibited increased amplitude of power spectra band traces during sleep states compared to waking states.

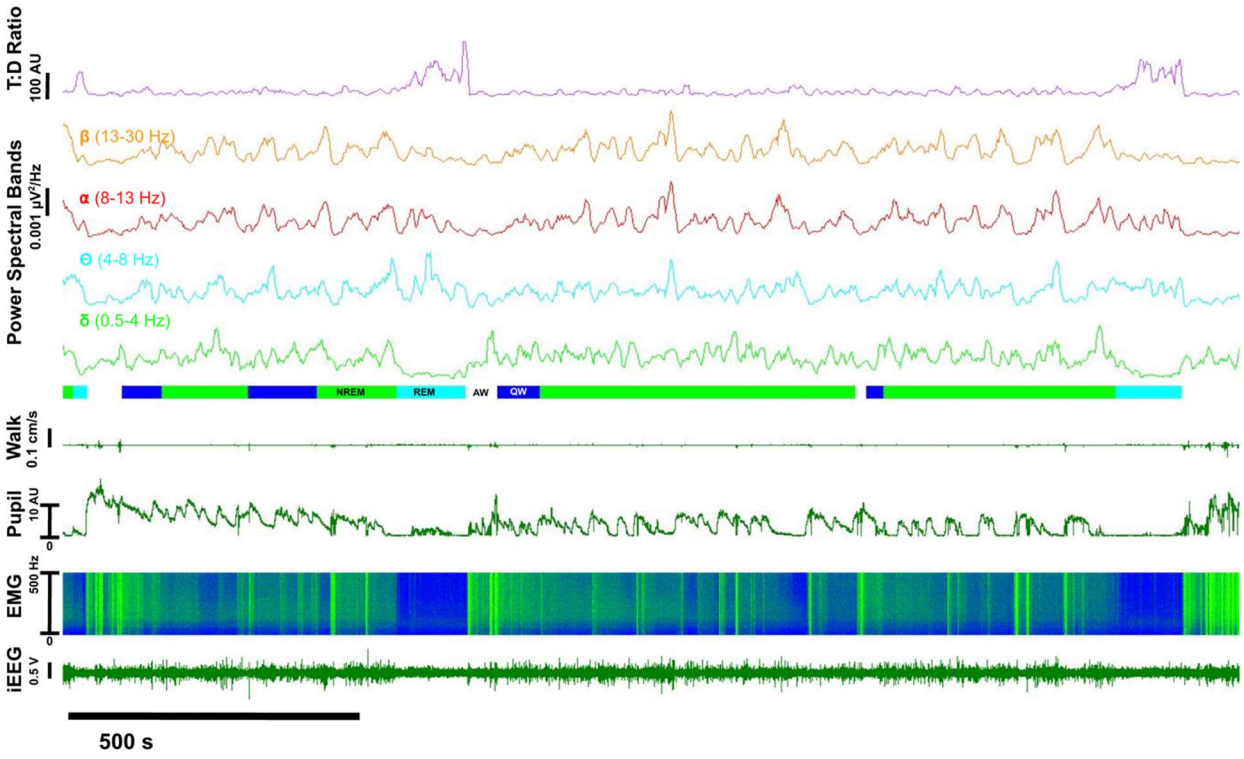


Figure 12: Representative Recording Session 2 with Separated Spectral Power Bands

2800 second sample from additional representative session with iEEG, EMG, Whisk, Walk, Pupil, power band spectra separated into individual channels (light green = delta, light blue = theta, red = alpha, orange = beta), T:D Ratio (purple), and arousal state epochs (light green = NREM, light blue = REM, dark blue = Quiet Wake, white = Active Wake). Further highlights coupling of behavioral metrics and patterns of spectral band activity to arousal state.

## Phase 2: The DOI-induced state contains mixed sleep-like and wake-like features

### *Wake-like Behavior with Sleep-like Neural Correlates*

As outlined above, canonical arousal states -- Active and Quiet Wake, NREM, and REM -- were reliably identified in control sessions using a multimodal approach including iEEG, EMG, pupil diameter, walking, and whisking behavior. The combination of these modalities provided reliable differentiation between high-arousal wake states and low-arousal sleep states, consistent with prior literature (Hulsey et al., 2024; McGinley et al., 2015; Reimer et al., 2016; Yüzgeç et al., 2018).

When post-DOI sessions were blindly scored using the same multimodal criteria, the dominant arousal state during the infra-slow pupil oscillation was most consistent with Active Wake and Quiet Wake states. This classification was largely due to the persistence of elevated muscle tone (high EMG activity) and a desynchronized mixed frequency iEEG profile that paralleled typical waking brain activity.

Despite this wake-like classification, a closer examination of the spectral content of the iEEG revealed key deviations from typical wakefulness. Specifically, during troughs of the ~0.03 Hz infra-slow pupil oscillation, we observed transient bursts of sigma (10-16 Hz) and theta (4-8 Hz) activity, which are features typically associated with NREM and REM sleep, respectively. These spectral features were not sufficient to support reclassification of the DOI-state as sleep, but their consistent emergence during the minima of the pupil is notable (Figure 13).

### *Anticorrelation of Sigma Power and Pupil Diameter*

Sigma power was anticorrelated with pupil diameter during both NREM and DOI infra-slow pupil oscillations (Figure 13), consistent with prior findings that suggest increased sigma

power reflects reduced noradrenergic tone (Osorio-Forero et al., 2021). As sigma oscillations have been proposed as an indicator of reduced arousal, their presence during an otherwise wake-like state suggests a transient dip in arousal or partial engagement of neural circuits typically reserved for sleep.

*Disruption of Sleep Cycles and Hybrid Arousal States*

At no point during the post-DOI recording sessions did mice transition into either NREM or REM sleep. This lack of REM in particular despite prolonged immobility and altered cortical dynamics suggests that DOI might suppress the brain's ability to engage in full sleep cycles, a previously reported effect of serotonergic psychedelics (Bréant et al., 2024; González et al., 2018; Souza et al., 2024; Thomas et al., 2022). This indicates that DOI might be inducing a disruption of the normal cycle of arousal states, and reinforces the notion that DOI produces a non-canonical state blurring the boundaries between sleep and wakefulness. The dissociation between behavioral and spectral state markers suggests that DOI might induce a hybrid state in which neural correlates of sleep partially emerge within an otherwise wake-like behavioral and physiological state. These results align with emerging models that suggest serotonergic psychedelics may disrupt or even reorganize global brain activity, destabilizing conventional state boundaries. This state falls outside the standard sleep-wake continuum, reflecting a pharmacologically induced alteration of arousal architecture.

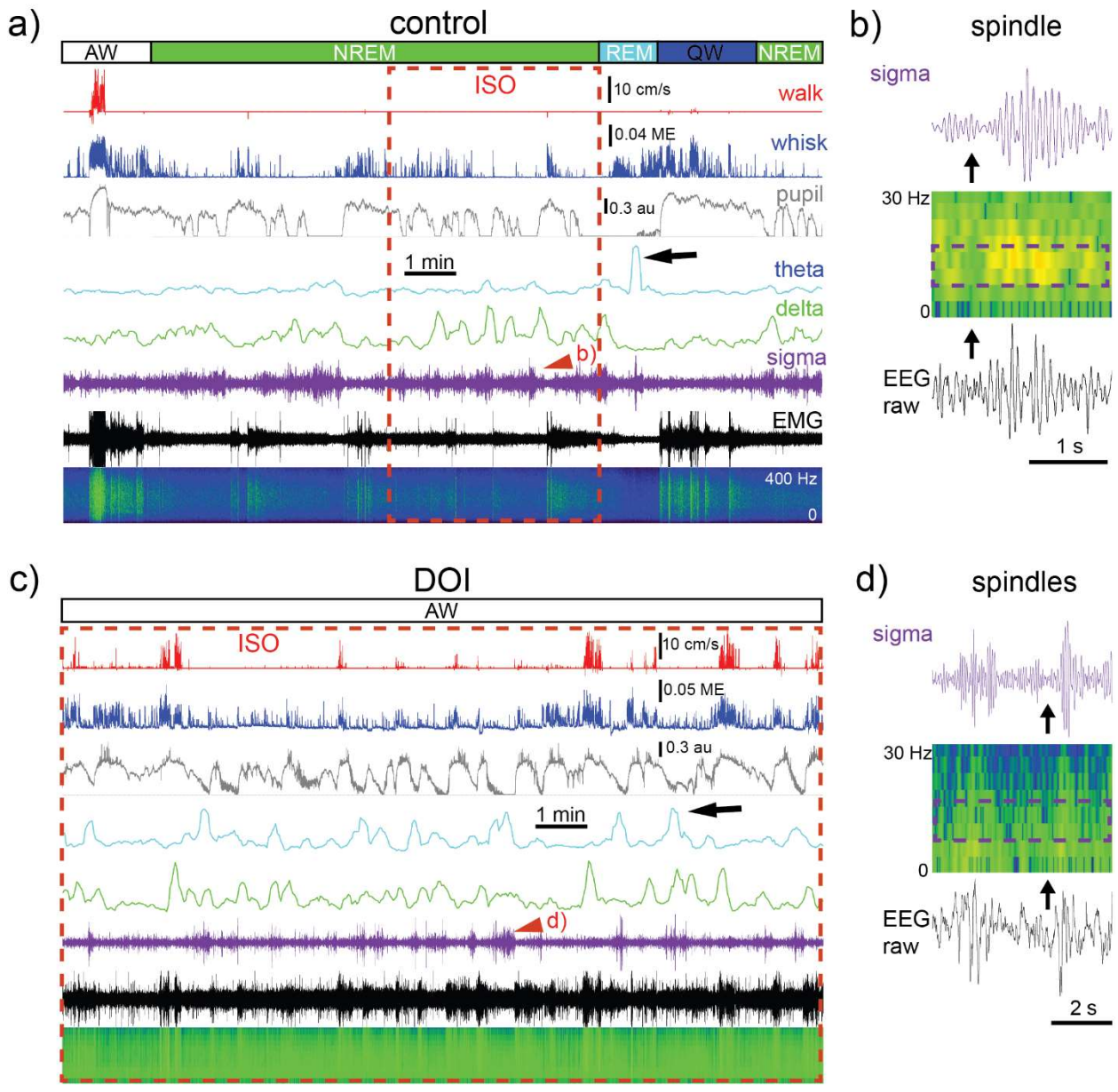
a)
control
AW
NREM
REM
QW
NREM
ISO
10 cm/s
walk
0.04 ME
whisk
pupil
0.3 au
1 min
theta
delta
b)
sigma
EMG
400 Hz
0
b)
spindle
sigma
30 Hz
0
EEG
raw
1 s
c)
DOI
AW
ISO
10 cm/s
0.05 ME
0.3 au
1 min
d)
d)
spindles
sigma
30 Hz
0
EEG
raw
2 s

Figure 13: Effect of 2,5-Dimethoxy-4-iodoamphetamine (DOI) on sleep/wake state transitions during spontaneous head-fixed behavior.

(**A**) Fifteen minutes of spontaneous behavior from control condition without DOI. Top colored boxes show sleep state scored by semi-automated analysis of intracranial electroencephalography (iEEG; single frontal electrode) and electromyography (single electrode in neck muscle). AW = Active Wake, QW = Quite Wake, NREM = Non-Rapid Eye Movement sleep, REM = Rapid Eye Movement sleep. Behavioral (walk speed, whisk motion energy, and pupil diameter) and electrical measurements (EMG raw trace and sonogram, bottom; iEEG-extracted theta (4 – 8 Hz) and delta (0.5 – 4 Hz) power, bandpass-filtered sigma (10-16 Hz) middle) are shown to be aligned to assigned arousal state. Dashed red box indicates period of infra-slow (0.01 - 0.1 Hz; ISO) pupil oscillations observed during NREM sleep, red arrowhead indicates identified sigma oscillation expanded in b), and black arrow indicates theta-band burst in iEEG during REM sleep. (**B**) Expanded spindle oscillation during ISO pupil trough of NREM sleep, from a). Raw iEEG shown at bottom, sonogram display of iEEG at middle, and 10-16 Hz band-pass filtered sigma oscillation at top. (**C**) Same as a, but ~40 min after administration of 10 mg/kg DOI injected subcutaneously. AW = Active Wake. Some ~5-10 s periods of ISO pupil troughs were identified as Quiet Wake from earlier in the session post-DOI. No REM sleep periods were identified during DOI sessions, but notable theta-band iEEG peaks were frequently observed during ISO pupil troughs. (**D**) same as b) but expanded from identified pupil oscillation (red arrowhead) in DOI session shown in c). Two spindle oscillations during ISO pupil trough of identified AW period are shown.

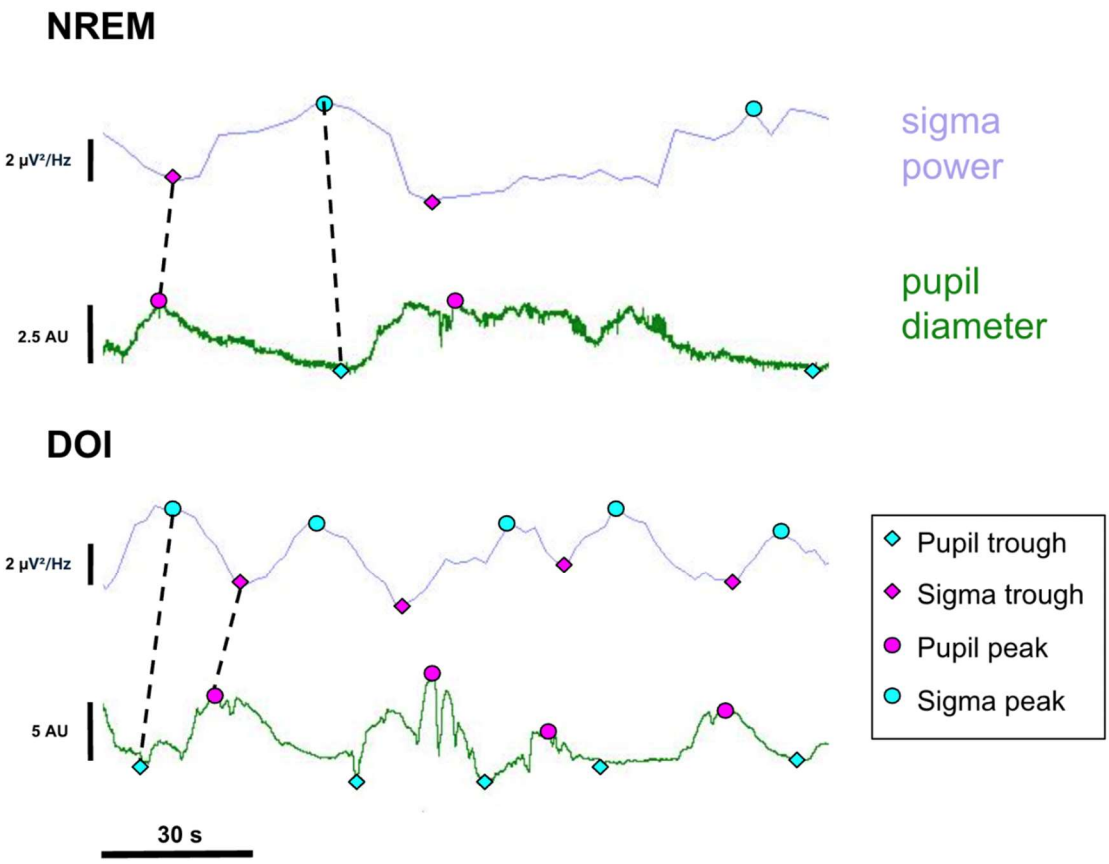


Figure 14: Sigma power anti-correlated to pupil diameter during NREM and DOI pupil ISOs

Top panel shows sigma power (purple) and pupil diameter (green) traces during NREM pupil ISO (infra-slow oscillation), bottom panel shows sigma power and pupil diameter during DOI pupil ISO. Circles were used to mark peaks and diamonds indicate troughs. Markers for sigma peaks and pupil troughs are magenta while markers for sigma troughs and pupil peaks are cyan. Dashed lines connect example markers illustrating the anti-correlation between pupil diameter and sigma power (i.e. when pupil diameter is high (peaks), sigma power is low (troughs) and vice-versa).

## Phase 3: Preliminary Imaging Supports Feasibility of Combining DOI Administration with Mesoscopic Imaging

### *Baseline Noradrenergic Activity and Behavioral Alignment*

Prior to DOI administration, baseline noradrenergic axon activity demonstrated expected alignment with behavioral markers including walking, whisking, and fluctuations in pupil diameter (Figure 15). These findings are consistent with previous studies demonstrating that noradrenergic activity is coupled to fluctuations in arousal state and sensorimotor activity (Anumba et al., 2024; Collins et al., 2023; Reimer et al., 2016). Behavioral activity -- specifically walking, whisking, and increasing pupil diameter -- reliably coincided with elevated fluorescent calcium activity in noradrenergic axons, which validates the reliability of our behavioral metrics and imaging paradigm.

### *Absence of Infra-Slow Pupil Oscillations Post-DOI*

Contrary to expectations based on previous sessions, the characteristic ~0.03 Hz infra-slow pupil oscillations were not observed following DOI injection during this session. In conjunction with the fact that this is a single session, the lack of the infra-slow pupil oscillation limited our ability to assess the hypothesized modulatory relationship between noradrenergic activity and these DOI-induced infra-slow oscillations. Without the presence of the oscillatory pupil activity, we were not able to determine whether noradrenergic activity exhibits phase-locked modulation as might be expected if the LC-NA system were fluctuating in tandem with these infra-slow oscillations.

There are multiple possible explanations for the absence of the expected pupil oscillations during this particular session. One plausible factor is a technical error in the subcutaneous DOI injection, possibly resulting in insufficient exposure to elicit the oscillatory signature.

Alternatively, it could be that the duration of the session was insufficient to facilitate the emergence of the infra-slow pupil oscillation, or that the animal was too aroused or insufficiently habituated. Regardless of the underlying cause, this session does not contain the data necessary to evaluate the role of noradrenaline during the DOI-induced infra-slow pupil oscillation.

*Validation of Methodology*

Despite the limitations, this session provided validation of the technical feasibility of combining widefield two-photon mesoscopic imaging with DOI pharmacological manipulation with a surgical preparation that allows for simultaneous recording from two intercranial electrodes for EEG recordings and a cranial window for the two-photon mesoscopic calcium imaging. These data demonstrate that noradrenergic axon imaging can be sustained across pre- and post- injection periods, planting the seed for more comprehensive experiments to map the interaction between psychedelic compounds and neuromodulatory circuits in real time. Future studies will be better positioned to assess how DOI influences the dynamics of the LC-NA system with appropriate replication and improved control of DOI injection delivery.

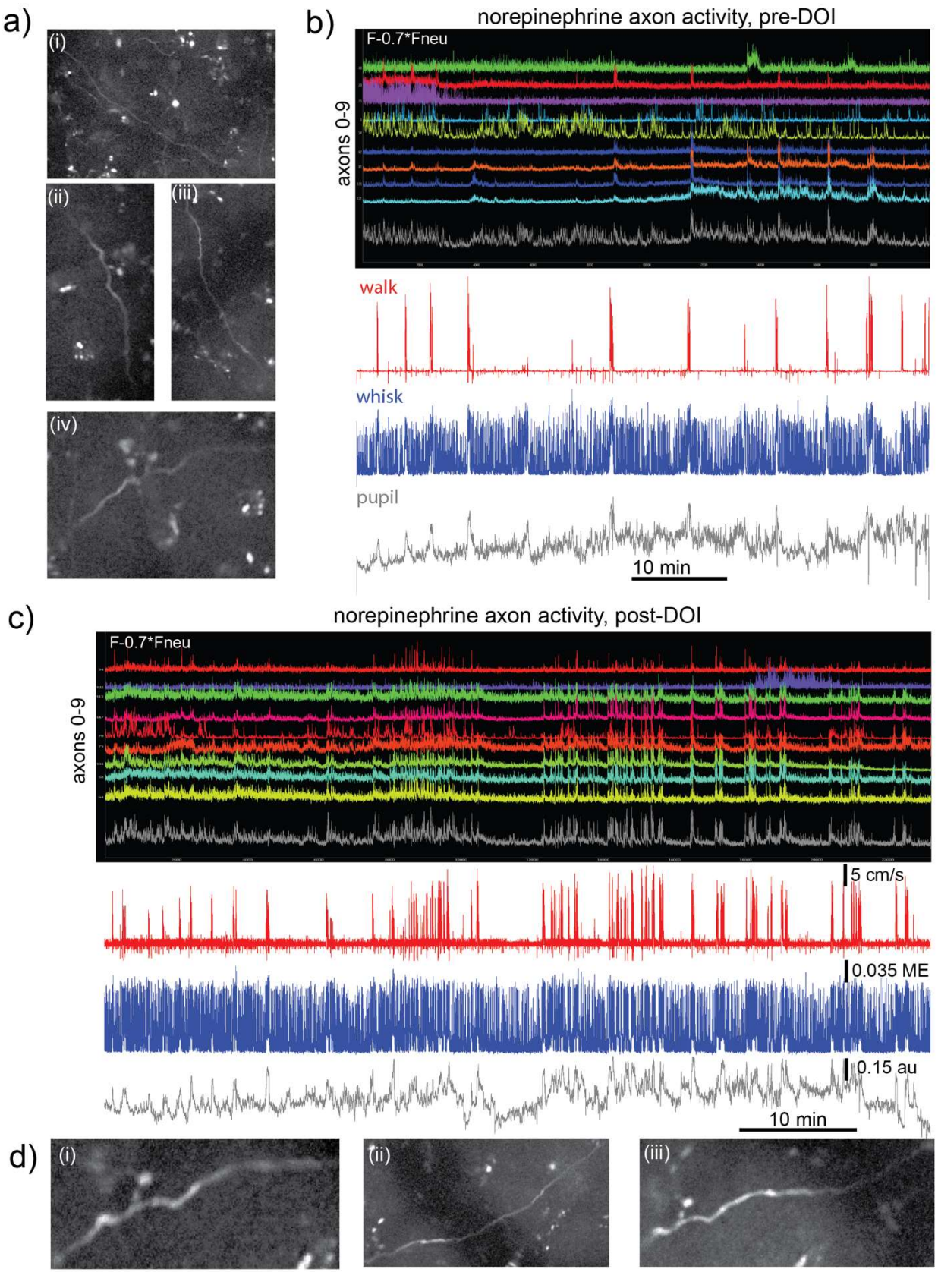
a)
(i)
(ii)
(iii)
(iv)
b)
norepinephrine axon activity, pre-DOI
F-0.7*Fneu
axons 0-9
walk
whisk
pupil
10 min
c)
norepinephrine axon activity, post-DOI
F-0.7*Fneu
axons 0-9
5 cm/s
0.035 ME
0.15 au
10 min
d)
(i)
(ii)
(iii)

Figure 15: Effect of 2,5-Dimethoxy-4-iodoamphetamine (DOI) on noradrenergic axon activity (DBH-Cre x GCaMP6s) during spontaneous behavior.

(**A**) Example sections of axons imaged in the dorsolateral cortex before administration of DOI, from the session shown in B. Axons were imaged at 5.55 Hz. (**B**) Neuropil subtracted fluorescence activity of 10 axons (top) shown aligned to walk speed, whisker motion energy, and pupil diameter (below). (**C**) Same as in B, but for a post-DOI session (10 mg/kg subcutaneous injection). (**D**) Same as in **A**, but example axons correspond to sessions shown in C.

# Discussion

This study sought to interrogate the effects of the psychedelic compound DOI on brain state dynamics, particularly in relation to canonical sleep-wake architecture. Utilizing multimodal metrics – intracranial electroencephalography (iEEG), electromyography (EMG), behavioral activity, pupil dynamics, and widefield calcium imaging – we were able to characterize arousal states in both control and DOI conditions.

## Emergence of Sleep-like Spectral Features During Wakefulness

During control sessions, canonical states of arousal (Active and Quiet Wake, NREM, and REM) were consistently identified using a combination of electrophysiological and behavioral signatures. After the administration of DOI, mice remained in wake-like neurobehavioral states characterized by sustained muscle tone, behavioral alertness, and a desynchronized iEEG profile. Of note, mice did not transition into REM sleep at any point during recordings following DOI administration, suggesting a disruption in typical sleep-wake cycling consistent with previous accounts of serotonergic psychedelics delaying or suppressing REM sleep (Bréant et al., 2024; González et al., 2018; Souza et al., 2024; Thomas et al., 2022). This would align with earlier work showing that DOI specifically suppresses REM sleep (Monti & Jantos, 2006).

Despite this overall waking state classification, spectral features typically associated with sleep states – namely increased activity in the sigma and theta power spectral bands – emerged during the troughs of the DOI-induced infra-slow (~0.03 Hz) pupil oscillations. Additionally, sigma power was inversely correlated with pupil diameter during infra-slow pupil oscillations in both NREM and DOI epochs, in line with the hypothesis that these oscillations reflect transient dips in arousal and noradrenergic activity. These findings are in line with previous studies showing that serotonergic psychedelics can induce sleep-like spectral attributes, such as slow-

wave and thalamocortical-spindle activity, in animals that otherwise appear to be in a waking state (Bréant et al., 2024; Souza et al., 2024). Building upon this, our results suggest that such features arise in temporal alignment with the ~0.03 Hz infra-slow pupil oscillations, which suggests the potential involvement of the LC-NA neuromodulatory system. The decoupling between behavioral and spectral markers implies that the DOI-induced state blurs the lines between endogenous sleep and wake arousal states, consistent with previous reports of DOI-inducing a decoupling or rearrangement of behavioral state and cortical activity (Olson et al., 2024)

**Insights From Preliminary Noradrenergic Axon Imaging During DOI**

In a complimentary imaging session, we used mesoscopic two-photon imaging to assess noradrenergic activity before and after the administration of DOI. Pre-DOI recordings demonstrated coupling of noradrenergic activity with behavioral arousal markers like walking, whisking, and pupillometry. However, counter to expectations, the hallmark ~0.03 infra-slow pupil oscillation was absent following DOI administration. This prevented direct evaluation of whether noradrenergic activity fluctuates in tandem with the rhythm of this oscillatory activity in this single session. Although the absence of the infra-slow pupil oscillation limits the extent of interpretation, the session still validates the achievability of using real-time neuroimaging techniques to evaluate the effects of pharmacological agents like DOI in a preparation that allows for simultaneous EEG and EMG recordings.

**Limitations and Future Directions**

This study has several limitations. For starters, our findings are based on a limited number of sessions and subject sample size (see Table 1). These underpowered results could be influenced by variability in drug administration and individual arousal baselines, as well as

individual differences in iEEG and EMG signals. Moreover, the absence of REM following DOI administration warrants further study to determine whether this observed effect is due to prolonged wakefulness, active suppression, or network destabilization. Future work should prioritize longitudinal recordings of both sleep and DOI sessions with the same subjects to improve confidence in the results. Moreover, although the multimodal approach to sleep-scoring facilitated detailed state classification, additional metrics like heart-rate variability would help to distinguish states more objectively, as would quantitative thresholds to distinguish between EMG tone for NREM and Quiet Wake states. Moreover, rigorous statistical analysis would also increase the reliability of claims about the effects of DOI on arousal state based on these data.

This project did not record both sleep and DOI-induced arousal states in the same individual animals, which would make for more compelling comparisons between the behavioral and electrophysiological features of the DOI-induced and canonical states of arousal. Ideally, future data acquisition would collect control sleep sessions prior to any DOI sessions from the same animals in order to enable a more direct comparison of NREM and DOI infra-slow oscillatory activity.

**A Hybrid or Dysregulated Arousal State?**

Altogether, these results suggest that the brain state induced by DOI represents an altered state characterized by a paradoxical combination of sleep- and wake-like features. Exhibiting behavioral wakefulness along with periodic sleep-like spectral features, this state may represent a pharmacologically dysregulated state of arousal in which cortical oscillations appear to be, at least intermittently, uncoupled from typical behavioral state transitions. Thorough examination of the dynamics of psychedelic-induced arousal states is increasingly important to understand the profound alterations in consciousness and perception that are achieved through the psychedelic

experience. This project aims to contribute to the growing body of work focusing on how psychedelics alter the experience of consciousness, as well as the fundamental architecture of arousal states. This cracks open the door for further investigation of how psychedelics interact with sleep-wake architecture and neuromodulatory systems, as well as whether these altered states have functional applicability in both psychiatric and basic neuroscience domains.

# Bibliography


*Animal Welfare Services | Research and Innovation*. (n.d.). Retrieved May 3, 2025, from https://research.uoregon.edu/about/administrative-units/research-integrity/animal-welfare-services

Anumba, N., Kelberman, M. A., Pan, W., Marriott, A., Zhang, X., Xu, N., Weinshenker, D., & Keilholz, S. (2024). The effects of locus coeruleus optogenetic stimulation on global spatiotemporal patterns in rats. *Imaging Neuroscience*, *2*, 1–20. https://doi.org/10.1162/imag_a_00314

Berridge, C. W. (2008). Noradrenergic modulation of arousal. *Brain Research Reviews*, *58*(1), 1–17. https://doi.org/10.1016/j.brainresrev.2007.10.013

Blier, P. (2001). Crosstalk between the norepinephrine and serotonin systems and its role in the antidepressant response. *Journal of Psychiatry & Neuroscience : JPN*, *26*(Suppl), S3-10.

Bréant, B. J. B., Mengual, J. P., Hoerder-Suabedissen, A., Patel, J., Bannerman, D. M., Sharp, T., & Vyazovskiy, V. V. (2024). *Sleep-like state during wakefulness induced by psychedelic 5-MeO-DMT in mice* (p. 2022.12.11.519886). bioRxiv. https://doi.org/10.1101/2022.12.11.519886

Breton-Provencher, V., Drummond, G. T., & Sur, M. (2021). Locus Coeruleus Norepinephrine in Learned Behavior: Anatomical Modularity and Spatiotemporal Integration in Targets. *Frontiers in Neural Circuits*, *15*. https://doi.org/10.3389/fncir.2021.638007

Buskila, Y., Bellot-Saez, A., & Morley, J. W. (2019). Generating Brain Waves, the Power of Astrocytes. *Frontiers in Neuroscience*, *13*. https://doi.org/10.3389/fnins.2019.01125

Calder, A. E., & Hasler, G. (2023). Towards an understanding of psychedelic-induced neuroplasticity. *Neuropsychopharmacology*, *48*(1), 104–112. https://doi.org/10.1038/s41386-022-01389-z

Calvey, T., & Howells, F. M. (2018). Chapter 1—An introduction to psychedelic neuroscience. In T. Calvey (Ed.), *Progress in Brain Research* (Vol. 242, pp. 1–23). Elsevier. https://doi.org/10.1016/bs.pbr.2018.09.013

Carro-Domínguez, M., Huwiler, S., Oberlin, S., Oesch, T. L., Badii, G., Lüthi, A., Wenderoth, N., Meissner, S. N., & Lustenberger, C. (2025). Pupil size reveals arousal level fluctuations in human sleep. *Nature Communications*, *16*(1), 2070. https://doi.org/10.1038/s41467-025-57289-5

Catterall, W. A. (n.d.). *The Molecular Basis of Neuronal Excitability | Science*. Retrieved April 24, 2025, from https://www.science.org/doi/abs/10.1126/science.6320365

Chang, M. C. J., & Grieder, F. B. (2024). The continued importance of animals in biomedical research. *Lab Animal*, *53*(11), 295–297. https://doi.org/10.1038/s41684-024-01458-4

Chen, T.-W., Wardill, T. J., Sun, Y., Pulver, S. R., Renninger, S. L., Baohan, A., Schreiter, E. R., Kerr, R. A., Orger, M. B., Jayaraman, V., Looger, L. L., Svoboda, K., & Kim, D. S. (2013). Ultrasensitive fluorescent proteins for imaging neuronal activity. *Nature*, *499*(7458), 295–300. https://doi.org/10.1038/nature12354

Collins, L., Francis, J., Emanuel, B., & McCormick, D. A. (2023). Cholinergic and noradrenergic axonal activity contains a behavioral-state signal that is coordinated across the dorsal cortex. *eLife*, *12*, e81826. https://doi.org/10.7554/eLife.81826

Craig, M., Ottaway, G., & Dewar, M. (2018). Rest on it: Awake quiescence facilitates insight. *Cortex*, *109*, 205–214. https://doi.org/10.1016/j.cortex.2018.09.009

del Castillo, J., & Katz, B. (1954). Quantal components of the end-plate potential. *The Journal of Physiology*, *124*(3), 560–573. https://doi.org/10.1113/jphysiol.1954.sp005129

Doss, M. K., Madden, M. B., Gaddis, A., Nebel, M. B., Griffiths, R. R., Mathur, B. N., & Barrett, F. S. (2022). Models of psychedelic drug action: Modulation of cortical-subcortical circuits. *Brain*, *145*(2), 441–456. https://doi.org/10.1093/brain/awab406

Francis, J. (2021). *The Relationship Between Cholinergic and Noradrenergic Activity and Behavioral State*. https://hdl.handle.net/1794/26516

Girardeau, G., & Lopes-dos-Santos, V. (2021). Brain neural patterns and the memory function of sleep. *Science*, *374*(6567), 560–564. https://doi.org/10.1126/science.abi8370

González, J., Prieto, J. P., Rodríguez, P., Cavelli, M., Benedetto, L., Mondino, A., Pazos, M., Seoane, G., Carrera, I., Scorza, C., & Torterolo, P. (2018). Ibogaine Acute Administration in Rats Promotes Wakefulness, Long-Lasting REM Sleep Suppression, and a Distinctive Motor Profile. *Frontiers in Pharmacology*, *9*. https://doi.org/10.3389/fphar.2018.00374

Gray, J. A., & Roth, B. L. (2001). Paradoxical trafficking and regulation of 5-HT2A receptors by agonists and antagonists. *Brain Research Bulletin*, *56*(5), 441–451. https://doi.org/10.1016/S0361-9230(01)00623-2

Gross, D., & Tolba, R. H. (2015). Ethics in Animal-Based Research. *European Surgical Research*, *55*(1–2), 43–57. https://doi.org/10.1159/000377721

Hermans, L. W. A., Huijben, I. A. M., van Gorp, H., Leufkens, T. R. M., Fonseca, P., Overeem, S., & van Gilst, M. M. (2022). Representations of temporal sleep dynamics: Review and synthesis of the literature. *Sleep Medicine Reviews*, *63*(101611), 101611. https://doi.org/10.1016/j.smrv.2022.101611

Hodgkin, A. L., & Katz, B. (1949). The effect of sodium ions on the electrical activity of the giant axon of the squid. *The Journal of Physiology*, *108*(1), 37–77. https://doi.org/10.1113/jphysiol.1949.sp004310

Hulsey, D., Zumwalt, K., Mazzucato, L., McCormick, D. A., & Jaramillo, S. (2024). Decision-making dynamics are predicted by arousal and uninstructed movements. *Cell Reports*, *43*(2). https://doi.org/10.1016/j.celrep.2024.113709

Jaster, A. M., & González-Maeso, J. (2023). Mechanisms and molecular targets surrounding the potential therapeutic effects of psychedelics. *Molecular Psychiatry*, *28*(9), 3595–3612. https://doi.org/10.1038/s41380-023-02274-x

Jones, B. E. (2005). Basic Mechanisms of Sleep-Wake States. *Principles and Practice of Sleep Medicine*, 136–153. https://doi.org/10.1016/b0-72-160797-7/50018-5

Joshi, S., Li, Y., Kalwani, R. M., & Gold, J. I. (2016). Relationships between Pupil Diameter and Neuronal Activity in the Locus Coeruleus, Colliculi, and Cingulate Cortex. *Neuron*, *89*(1), 221–234. https://doi.org/10.1016/j.neuron.2015.11.028

Kaplan, J. (1988). The Use of Animals in Research. *Science*, *242*(4880), 839–840. https://doi.org/10.1126/science.3187522

Koshmanova, E., Berger, A., Beckers, E., Campbell, I., Mortazavi, N., Sharifpour, R., Paparella, I., Balda, F., Berthomier, C., Degueldre, C., Salmon, E., Lamalle, L., Bastin, C., Van Egroo, M., Phillips, C., Maquet, P., Collette, F., Muto, V., Chylinski, D., … Vandewalle, G. (n.d.). Locus coeruleus activity while awake is associated with REM sleep quality in older individuals. *JCI Insight*, *8*(20), e172008. https://doi.org/10.1172/jci.insight.172008

Kropotov, J. D. (2022). The enigma of infra-slow fluctuations in the human EEG. *Frontiers in Human Neuroscience*, *16*. https://doi.org/10.3389/fnhum.2022.928410

Lázár, Z. I., Dijk, D.-J., & Lázár, A. S. (2019). Infraslow oscillations in human sleep spindle activity. *Journal of Neuroscience Methods*, *316*, 22–34. https://doi.org/10.1016/j.jneumeth.2018.12.002

Lecci, S., Fernandez, L. M. J., Weber, F. D., Cardis, R., Chatton, J.-Y., Born, J., & Lüthi, A. (2017). Coordinated infraslow neural and cardiac oscillations mark fragility and offline periods in mammalian sleep. *Science Advances*, *3*(2), e1602026. https://doi.org/10.1126/sciadv.1602026

Lee, S.-H., & Dan, Y. (2012). Neuromodulation of Brain States. *Neuron*, *76*(1), 209–222. https://doi.org/10.1016/j.neuron.2012.09.012

Loewi, O. (1945). Chemical Transmission of Nerve Impulses. *American Scientist*, *33*(3), 159–174.

López-Rubalcava, C., & Fernández-Guasti, A. (1994). Noradrenaline-serotonin interactions in the anxiolytic effects of 5-HT1A agonists. *Behavioural Pharmacology*, *5*(1), 42.

Maćkowiak, M. (2023). Psychedelics action and schizophrenia. *Pharmacological Reports*, *75*(6), 1350–1361. https://doi.org/10.1007/s43440-023-00546-5

Maheu, M., Donner, T. H., & Wiegert, J. S. (2025). *Serotonergic and Noradrenergic Interactions in Pupil-linked Arousal* (p. 2025.03.26.644382). bioRxiv. https://doi.org/10.1101/2025.03.26.644382

McCormick, D. A., Nestvogel, D. B., & He, B. J. (2020). Neuromodulation of Brain State and Behavior. *Annual Review of Neuroscience*, *43*(Volume 43, 2020), 391–415. https://doi.org/10.1146/annurev-neuro-100219-105424

McGinley, M. J., Vinck, M., Reimer, J., Batista-Brito, R., Zagha, E., Cadwell, C. R., Tolias, A. S., Cardin, J. A., & McCormick, D. A. (2015). Waking State: Rapid Variations Modulate Neural and Behavioral Responses. *Neuron*, *87*(6), 1143–1161. https://doi.org/10.1016/j.neuron.2015.09.012

Monti, J. M., & Jantos, H. (2006). Effects of the serotonin 5-HT2A/2C receptor agonist DOI and of the selective 5-HT2A or 5-HT2C receptor antagonists EMD 281014 and SB-243213, respectively, on sleep and waking in the rat. *European Journal of Pharmacology*, *553*(1), 163–170. https://doi.org/10.1016/j.ejphar.2006.09.027

Nardou, R., Sawyer, E., Song, Y. J., Wilkinson, M., Padovan-Hernandez, Y., de Deus, J. L., Wright, N., Lama, C., Faltin, S., Goff, L. A., Stein-O'Brien, G. L., & Dölen, G. (2023). Psychedelics reopen the social reward learning critical period. *Nature*, *618*(7966), 790–798. https://doi.org/10.1038/s41586-023-06204-3

Nelson, A., & Mooney, R. (2016). The Basal Forebrain and Motor Cortex Provide Convergent yet Distinct Movement-Related Inputs to the Auditory Cortex. *Neuron*, *90*(3), 635–648. https://doi.org/10.1016/j.neuron.2016.03.031

Olson, R. J., Bartlett, L., Sonneborn, A., Milton, R., Bretton-Granatoor, Z., Firdous, A., Harris, A. Z., & Abbas, A. I. (2024). Decoupling of cortical activity from behavioral state following administration of the classic psychedelic DOI. *Neuropharmacology*, *257*, 110030. https://doi.org/10.1016/j.neuropharm.2024.110030

Osorio-Forero, A., Cardis, R., Vantomme, G., Guillaume-Gentil, A., Katsioudi, G., Devenoges, C., Fernandez, L. M. J., & Lüthi, A. (2021). Noradrenergic circuit control of non-REM sleep substates. *Current Biology*, *31*(22), 5009-5023.e7. https://doi.org/10.1016/j.cub.2021.09.041

Osorio-Forero, A., Foustoukos, G., Cardis, R., Cherrad, N., Devenoges, C., Fernandez, L. M. J., & Lüthi, A. (2025). Infraslow noradrenergic locus coeruleus activity fluctuations are gatekeepers of the NREM–REM sleep cycle. *Nature Neuroscience*, *28*(1), 84–96. https://doi.org/10.1038/s41593-024-01822-0

Osuchowski, M. F., Remick, D. G., Lederer, J. A., Lang, C. H., Aasen, A. O., Aibiki, M., Azevedo, L. C., Bahrami, S., Boros, M., Cooney, R., Cuzzocrea, S., Jiang, Y., Junger, W. G., Hirasawa, H., Hotchkiss, R. S., Li, X.-A., Radermacher, P., Redl, H., Salomao, R., … Chaudry, I. H. (2014). Abandon the Mouse Research Ship? Not Just Yet! *Shock*, *41*(6), 463. https://doi.org/10.1097/SHK.0000000000000153

Pachitariu, M., Stringer, C., Dipoppa, M., Schröder, S., Rossi, L. F., Dalgleish, H., Carandini, M., & Harris, K. D. (2017). *Suite2p: Beyond 10,000 neurons with standard two-photon microscopy* (p. 061507). bioRxiv. https://doi.org/10.1101/061507

Pape, H.-C., & McCormick, D. A. (1989). Noradrenaline and serotonin selectively modulate thalamic burst firing by enhancing a hyperpolarization-activated cation current. *Nature*, *340*(6236), 715–718. https://doi.org/10.1038/340715a0

Patel, A. K., Reddy, V., Shumway, K. R., & Araujo, J. F. (2025). Physiology, Sleep Stages. In *StatPearls*. StatPearls Publishing. http://www.ncbi.nlm.nih.gov/books/NBK526132/

Poe, G. R., Foote, S., Eschenko, O., Johansen, J. P., Bouret, S., Aston-Jones, G., Harley, C. W., Manahan-Vaughan, D., Weinshenker, D., Valentino, R., Berridge, C., Chandler, D. J., Waterhouse, B., & Sara, S. J. (2020). Locus coeruleus: A new look at the blue spot. *Nature Reviews Neuroscience*, *21*(11), 644–659. https://doi.org/10.1038/s41583-020-0360-9

Reimer, J., McGinley, M. J., Liu, Y., Rodenkirch, C., Wang, Q., McCormick, D. A., & Tolias, A. S. (2016). Pupil fluctuations track rapid changes in adrenergic and cholinergic activity in cortex. *Nature Communications*, *7*(1), 13289. https://doi.org/10.1038/ncomms13289

National Academy of Sciences. Research, N. A. of S. (US) and I. of M. (US) C. on the U. of A. in. (1991a). Preface. In *Science, Medicine, and Animals*. National Academies Press (US). https://www.ncbi.nlm.nih.gov/books/NBK223355/

Smetters, D., Majewska, A., & Yuste, R. (1999). Detecting Action Potentials in Neuronal Populations with Calcium Imaging. *Methods*, *18*(2), 215–221. https://doi.org/10.1006/meth.1999.0774

Sofroniew, N. J. (2017). Q&A: The brain under a mesoscope: the forest and the trees. *BMC Biology*, *15*(1), 82. https://doi.org/10.1186/s12915-017-0426-y

Sofroniew, N. J., Flickinger, D., King, J., & Svoboda, K. (2016). A large field of view two-photon mesoscope with subcellular resolution for in vivo imaging. *eLife*, *5*, e14472. https://doi.org/10.7554/eLife.14472

Souza, A. C., Souza, B. C., França, A., Moradi, M., Souza, N. C., Leão, K. E., Tort, A. B. L., Leão, R. N., Lopes-dos-Santos, V., & Ribeiro, S. (2024). 5-MeO-DMT induces sleep-like LFP spectral signatures in the hippocampus and prefrontal cortex of awake rats. *Scientific Reports*, *14*(1), 11281. https://doi.org/10.1038/s41598-024-61474-9

Stevner, A. B. A., Vidaurre, D., Cabral, J., Rapuano, K., Nielsen, S. F. V., Tagliazucchi, E., Laufs, H., Vuust, P., Deco, G., Woolrich, M. W., Van Someren, E., & Kringelbach, M. L. (2019). Discovery of key whole-brain transitions and dynamics during human wakefulness and non-REM sleep. *Nature Communications*, *10*(1), 1035. https://doi.org/10.1038/s41467-019-08934-3

Stosiek, C., Garaschuk, O., Holthoff, K., & Konnerth, A. (2003). In vivo two-photon calcium imaging of neuronal networks. *Proceedings of the National Academy of Sciences*, *100*(12), 7319–7324. https://doi.org/10.1073/pnas.1232232100

Swift, K. M., Gross, B. A., Frazer, M. A., Bauer, D. S., Clark, K. J. D., Vazey, E. M., Aston-Jones, G., Li, Y., Pickering, A. E., Sara, S. J., & Poe, G. R. (2018). Abnormal Locus Coeruleus Sleep Activity Alters Sleep Signatures of Memory Consolidation and Impairs Place Cell Stability and Spatial Memory. *Current Biology*, *28*(22), 3599-3609.e4. https://doi.org/10.1016/j.cub.2018.09.054

Tagliazucchi, E., Carhart-Harris, R., Leech, R., Nutt, D., & Chialvo, D. R. (2014). Enhanced repertoire of brain dynamical states during the psychedelic experience. *Human Brain Mapping*, *35*(11), 5442–5456. https://doi.org/10.1002/hbm.22562

Thomas, C. W., Blanco-Duque, C., Bréant, B. J., Goodwin, G. M., Sharp, T., Bannerman, D. M., & Vyazovskiy, V. V. (2022). Psilocin acutely alters sleep-wake architecture and cortical brain activity in laboratory mice. *Translational Psychiatry*, *12*(1), 1–13. https://doi.org/10.1038/s41398-022-01846-9

Turner, K. L., Gheres, K. W., & Drew, P. J. (2023). Relating Pupil Diameter and Blinking to Cortical Activity and Hemodynamics across Arousal States. *Journal of Neuroscience*, *43*(6), 949–964. https://doi.org/10.1523/JNEUROSCI.1244-22.2022

van Elk, M., & Yaden, D. B. (2022). Pharmacological, neural, and psychological mechanisms underlying psychedelics: A critical review. *Neuroscience & Biobehavioral Reviews*, *140*, 104793. https://doi.org/10.1016/j.neubiorev.2022.104793

Vickers, E. (2025, January 25). *Altered compositionality of cortical neural activity during psychedelic administration: Infraslow oscillations (~0.03 Hz)*. Institute of Neuroscience Winter Brain Talk, University of Oregon.

Vickers, E. D., & McCormick, D. A. (2024). Pan-cortical 2-photon mesoscopic imaging and neurobehavioral alignment in awake, behaving mice. *eLife*, *13*, RP94167. https://doi.org/10.7554/eLife.94167

Wallach, J., Cao, A. B., Calkins, M. M., Heim, A. J., Lanham, J. K., Bonniwell, E. M., Hennessey, J. J., Bock, H. A., Anderson, E. I., Sherwood, A. M., Morris, H., de Klein, R., Klein, A. K., Cuccurazzu, B., Gamrat, J., Fannana, T., Zauhar, R., Halberstadt, A. L., & McCorvy, J. D. (2023). Identification of 5-HT2A receptor signaling pathways associated with psychedelic potential. *Nature Communications*, *14*(1), 8221. https://doi.org/10.1038/s41467-023-44016-1

Warren, M. (2019). Night-vision 'super-mice' created using light-converting nanoparticles. *Nature*, *567*(7746), 16–17. https://doi.org/10.1038/d41586-019-00735-4

Watson, B. O. (2018). Cognitive and Physiologic Impacts of the Infraslow Oscillation. *Frontiers in Systems Neuroscience*, *12*. https://doi.org/10.3389/fnsys.2018.00044

Watson, B. O., Levenstein, D., Greene, J. P., Gelinas, J. N., & Buzsáki, G. (2016). Network Homeostasis and State Dynamics of Neocortical Sleep. *Neuron*, *90*(4), 839–852. https://doi.org/10.1016/j.neuron.2016.03.036

Weiss, E., Liu, Y., & Wang, Q. (2025). *The contribution of the locus coeruleus – norepinephrine system to the coupling between pupil-linked arousal and cortical state* (p. 2025.05.07.652771). bioRxiv. https://doi.org/10.1101/2025.05.07.652771

Xiang, L., Harel, A., Todorova, R., Gao, H., Sara, S. J., & Wiener, S. I. (2023). Locus coeruleus noradrenergic neurons phase-lock to prefrontal and hippocampal infra-slow rhythms that synchronize to behavioral events. *Frontiers in Cellular Neuroscience*, *17*. https://doi.org/10.3389/fncel.2023.1131151

Xu, M., Chung, S., Zhang, S., Zhong, P., Ma, C., Chang, W.-C., Weissbourd, B., Sakai, N., Luo, L., Nishino, S., & Dan, Y. (2015). Basal forebrain circuit for sleep-wake control. *Nature Neuroscience*, *18*(11), 1641–1647. https://doi.org/10.1038/nn.4143

Yamabe, M., Horie, K., Shiokawa, H., Funato, H., Yanagisawa, M., & Kitagawa, H. (2019). MC-SleepNet: Large-scale Sleep Stage Scoring in Mice by Deep Neural Networks. *Scientific Reports*, *9*(1), 15793. https://doi.org/10.1038/s41598-019-51269-8

Yüzgeç, Ö., Prsa, M., Zimmermann, R., & Huber, D. (2018). Pupil Size Coupling to Cortical States Protects the Stability of Deep Sleep via Parasympathetic Modulation. *Current Biology*, *28*(3), 392-400.e3. https://doi.org/10.1016/j.cub.2017.12.049

Zagha, E., & McCormick, D. A. (2014). Neural control of brain state. *Current Opinion in Neurobiology*, *29*, 178–186. https://doi.org/10.1016/j.conb.2014.09.010